Review

Recent Developments on CO₂ Hydrogenation Performance over Structured Zeolites: A Review on Properties, Synthesis, and Characterization

Methene Briones Cutad [1] , Mohammed J. Al-Marri [1,2,*] and Anand Kumar [1,*]

1 Department of Chemical Engineering, College of Engineering, Qatar University, Doha P.O. Box 2713, Qatar; mcutad@qu.edu.qa

2 Gas Processing Center, College of Engineering, Qatar University, Doha P.O. Box 2713, Qatar

* Correspondence: m.almarri@qu.edu.qa (M.J.A.-M.); akumar@qu.edu.qa (A.K.); Tel.: +974-44034146 (M.J.A.-M.)

Abstract: This review focuses on an extensive synopsis of the recent improvements in CO₂ hydrogenation over structured zeolites, including their properties, synthesis methods, and characterization. Key features such as bimodal mesoporous structures, surface oxygen vacancies, and the Si/Al ratio are explored for their roles in enhancing catalytic activity. Additionally, the impact of porosity, thermal stability, and structural integrity on the performance of zeolites, as well as their interactions with electrical and plasma environments, are discussed in detail. The synthesis of structured zeolites is analyzed by comparing the advantages and limitations of bottom-up methods, including hard templating, soft templating, and non-templating approaches, to top-down methods, such as dealumination, desilication, and recrystallization. The review addresses the challenges associated with these synthesis techniques, such as pore-induced diffusion limitations, morphological constraints, and maintaining crystal integrity, highlighting the need for innovative solutions and optimization strategies. Advanced characterization techniques are emphasized as essential for understanding the catalytic mechanisms and dynamic behaviors of zeolites, thereby facilitating further research into their efficient and effective use. The study concludes by underscoring the importance of continued research to refine synthesis and characterization methods, which is crucial for optimizing catalytic activity in CO₂ hydrogenation. This effort is important for achieving selective catalysis and is paramount to the global initiative to reduce carbon emissions and address climate change.

Keywords: carbon dioxide hydrogenation; structured zeolites; zeolites synthesis and characterization

1. Introduction

Global warming is a significant concern as it is exacerbated by the excessive emissions of greenhouse gases, specifically carbon dioxide (CO₂), which contribute to mounting climate-related issues [1]. CO₂ hydrogenation is gradually emerging as a critical technology for carbon neutrality, which provides a route for CO₂ valorization into valuable chemicals and fuels [2,3]. The process offers a two-fold solution; besides addressing the pivotal issue of CO₂ emissions, it also assists in the sustainable production of heavy hydrocarbons [4]. The selective and optimized transformation of CO₂ represents a current challenge considering its thermodynamic stability and inert properties [5].

There are two primary methods for converting CO₂ into hydrocarbons, both of which have also been industrially applied for decades, reflecting their proven scalability and commercial viability. The first method, modified Fischer–Tropsch synthesis (modified-FTS), combines the reverse water-gas shift (RWGS) reaction and the Fischer–Tropsch reaction [6]. This process not only synergistically utilizes CO₂ but also transforms it into various hydrocarbons, as evidenced by the long-standing operation of SASOL plants in South Africa and the ORYX GTL plant in Qatar, which all utilize FTS technology [7,8]. The second

method is the methanol-mediated route, where CO_2 is first converted into methanol and then transformed into hydrocarbons through the methanol-to-hydrocarbon (MTH) process. This pathway is exemplified by the operation of the world's largest methanol plant in Iran, which uses CO_2 as a feedstock [9]. Given the thermal hydrogenation foundation of both technologies, unless otherwise stated, this review will therefore primarily focus on the thermal hydrogenation of CO_2. This approach has been comprehensively explored over structured zeolites in terms of mechanisms, kinetics, catalyst development, and industrial improvements and applications, as reviewed extensively by Ye et al. [10], Ojelade and Zaman [11], and Wang et al. [12], who have detailed the underlying processes and implementations of both the modified-FTS and MTH routes. Structured zeolites, with their unequaled porous structures and acid-base properties, are used as catalysts in a whole range of chemical processes, among them CO_2 hydrogenation. Figure 1 shows the classes of well-known zeolites (e.g., natural [13], and synthetic [14–16]). Both zeolite types have been widely applied not just in catalysis [17], but even in other industries such as water and wastewater treatment, agriculture, biomedicine, laundry detergents, and construction [18–22].
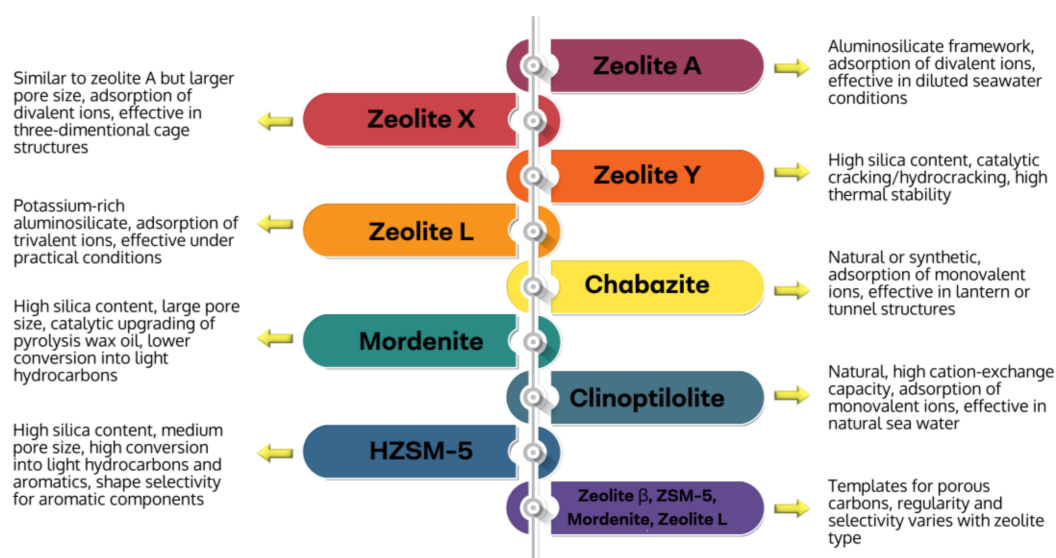

Figure 1. Types of zeolites and their synthesis, application, and performance.

For CO_2 hydrogenation, zeolite application has received considerable attention over the last decade. Figure 2 shows the distribution of several articles displayed on Google Scholar when the phrase "CO_2 hydrogenation over zeolites" is used to search articles. The trend indicates unprecedented growth in the application of zeolites for CO_2 conversion reactions, particularly over the last decade, where an exponential trend has been seen. The recent signs of progress have mainly concentrated on the improvement of the zeolites through careful control of their compositions, porous characteristics, and coupling of thermal and mechanical properties that render promotion of reaction selectivity and enhance the production of longer-chained hydrocarbons such as aromatics, liquid fuels, alcohols, and heavy olefins [5,23]. It should be noted that zeolites by themselves have been widely studied for various applications as aforementioned; nonetheless, the recent developments in the field of CO_2 catalysis and the growing interest of researchers in the application of zeolites for CO_2 conversion create a demand for a review covering the growth in the field, primarily over the last decade, which is the motivation behind this article. This study intends to summarize the recent advances in the area of CO_2 hydrogenation over structured zeolites by offering a synoptic view of the different influential parameters, synthesis techniques, characterization requirements, and catalytic functions. The review critically evaluates the current literature that should bring out new ideas, findings of key innovations, and significant breakthroughs.

It will embrace the rudiments of the process, the specific traits of structured zeolites, and their role in augmenting catalytic activity. In addition, there will be reflections on the challenges and prospects in this field; hence, one can get ideas on structured zeolites and the way they may be used to reduce the global CO_2 problem.
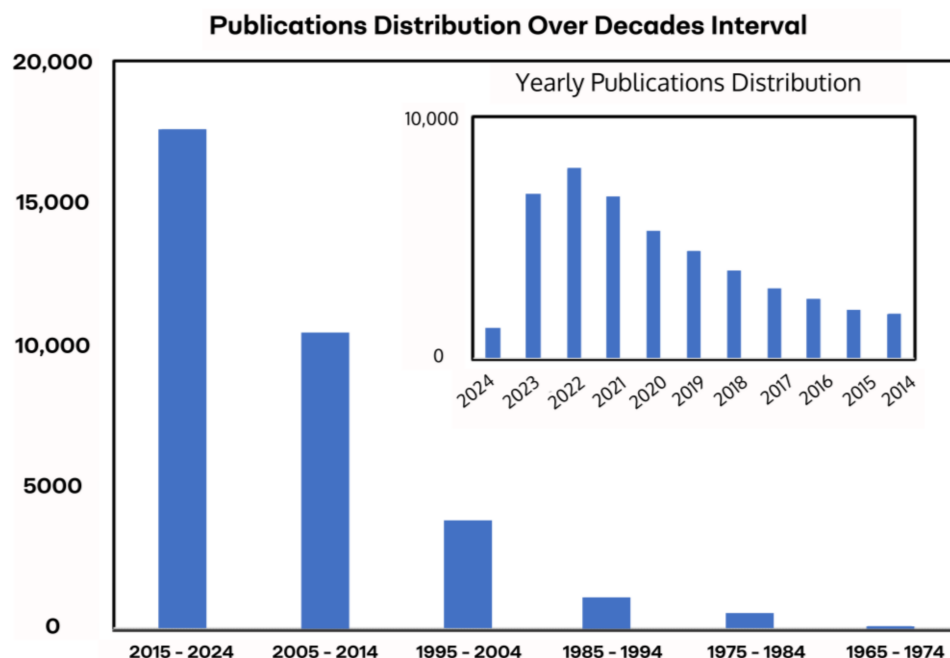

Figure 2. Number of publications displayed by Google Scholar search using the phrase "CO_2 Hydrogenation over zeolites".

2. Thermal CO_2 Hydrogenation over Other Methods: A Brief Overview

In addition to the well-established thermal routes for CO_2 hydrogenation, such as FTS and MTH mentioned in the introduction section, various alternative methods have been explored to expand the range of technologies for CO_2 reduction. Table 1 shows the alternatives, which include electrochemical, photocatalytic, biochemical, and chemo-enzymatic methods, each characterized by distinct mechanisms and specific applications. While each technology has its own merits and limitations, its implementation in industries largely depends on the type of industry, the purity level of the product, and the scale of processing.

Table 1. State-of-the-art overview of CO_2 hydrogenation technologies: assessing advantages and limitations.

Method	Advantages	Disadvantages
Thermal [10–12]	Proven scalability, high product yields, extensively used in industrial settings	Can be energy-intensive; less environmentally friendly without renewable energy integration; catalyst stability issues
Electrochemical [24,25]	Facilitates CO_2 reduction using electricity, can be integrated with renewable electricity sources; scalable; stable long-term	Often a broad product distribution at high conversions; high energy demand; economically challenging
Photocatalytic [26,27]	Utilizes sunlight, environmentally friendly; no need for external energy inputs; economically feasible	Lower efficiency and stability, which hinders scalability; lower yields
Biochemical and Chemo-enzymatic [28–30]	High selectivity; operates under mild conditions; efficient for producing bulk chemicals	Slow reaction rates; complex maintenance of biocatalytic activity; high temperatures can inhibit enzyme activity

However, despite the diversity of available technologies, the foundation of hydrocarbon processing industrial plants still predominantly relies on thermal conversion methods. This is not only evident in traditional sectors like chemical synthesis via the FTS and MTH routes but is also a staple in the oil and gas industries. Processes such as Gas to Liquid (GTL) and Natural Gas Reforming (NGR) for hydrogen production extensively employ thermal methods due to their robustness and scalability [31,32]. These processes are integral to the production workflows in these industries, underlining the predominance of thermal techniques.

The thermal CO_2 hydrogenation process appears more energy-efficient than the solar route. For example, the thermal method benefits from a novel membrane reactor that enhances methanol yield and requires a smaller reactor, which exhibits superior energy efficiency at 70.3% [33]. In contrast, a solar CO_2 hydrogenation process achieves an energy efficiency of 15.5%, with a 26% improvement over such previous methods possible under optimal conditions [34]. Despite the advancements in solar hydrogenation, the thermal approach is suggested to be superior in terms of energy efficiency. This sharp contrast highlights the larger energy savings characteristic of thermal CO_2 hydrogenation. In addition, Zeng et al. [35] highlighted that plasma power (a form of thermal hydrogenation) is more efficient than heating power (a form of solar hydrogenation), even at lower temperatures, showing the highest conversions in the presence of plasma.

Unlike thermal processes, electrochemical processes are energy-intensive, and the lifespan of catalytic materials is low for such processes [36]. Hence, the application of electrochemical conversion in industries remains limited, even today, due to practical challenges in optimizing key parameters such as Faradaic efficiency (FE), Energetic Efficiency (EE), and Current Density (CD), which are crucial for the success of this approach [37,38]. To overcome these obstacles, catalysts must possess rapid electron transmission capabilities, superior electron transport ability, and robust electron-transporting features [36,39].

The primary distinction between photocatalytic CO_2 reduction and electrochemical CO_2 reduction is in their electron sources. In photocatalytic reduction, electrons are generated by exposing semiconductors to light, whereas in electrochemical reduction, electrons are sourced through the application of an electrical current. However, since photocatalytic methods depend on light absorption, they often suffer from limited efficiency, poor selectivity, and insufficient product variety [40]. In addition, such processes are intricate, encompassing various mechanisms like electron and proton transfer as well as the formation and breaking of chemical bonds, which remain poorly comprehended [37]. Furthermore, the process of photocatalytic conversion necessitates substantial capital investment and energy, especially when using semiconductors with wide band gaps [41]. Substantial challenges in substrate-based photocatalysts include the degradation of polymers, the creation of volatile by-products, and the complexities in separating the catalyst from the final product [41]. Therefore, the catalysts used in such a conversion process need to be optimized and treated, which can additionally increase the overall expenses [42].

Biochemical and chemo-enzymatic methods, though innovative and sustainable, face challenges due to the high cost of cofactors, and complex biological systems and demand a need for efficient cofactor regeneration for large-scale applications [43,44]. One of the challenges that the biochemical conversion process faces is the maintenance of an adequate nutrient supply, the collection of end products, and the sustainability of the microbial cultures. It has been suggested that genetic modification of these organisms could overcome such problems [43]. However, this approach can fail in some cases, as the insertion of many gene copies can accidentally inactivate some genes—a situation called genetic knockout [41]. Hence, pretreatment is required, and productivity is lower when compared to that of the thermo-chemical process. Generally, enzymes, often costly and characterized by limited stability, activity, and reusability, face constraints in their industrial usage. Technologies like enzyme modification and immobilization require further advancement to decrease costs and boost enzyme performance and recyclability, thereby enhancing economic viability [45]. Additionally, the slow reaction rate significantly hinders the industrial application of

enzymatic CO_2 conversion, necessitating the deployment of biocatalysts to address kinetic issues and achieve a faster, more effective conversion process.

Therefore, considering the extensive application, proven scalability, and integration within the hydrocarbon industrial processes, the thermal route remains the preferred method for CO_2 hydrogenation due to its robustness and higher reaction rates, especially when efficiency and selectivity are paramount. This assertion is corroborated by the above case studies, which clearly illustrated the limitations inherent in alternative methods and the comparative strengths of the thermal approach. Drawing upon these insights, Table 2 encapsulates the array of advantages that thermal methods hold over their electrochemical, photocatalytic, biochemical, and chemo-enzymatic counterparts.

Table 2. Efficacy of thermal conversion against electrochemical, photocatalytic, biochemical, and chemo-enzymatic methods in CO_2 hydrogenation.

Hydrogenation Feature	Thermal Conversion [33–35]	Electrochemical Conversion [36–39]	Photocatalytic Conversion [37,40–42]	Biochemical and Chemo-Enzymatic Conversion [41,43–45]
Energy Efficiency	High, but varies based on the used catalytic materials	Energy-intensive with usually low catalytic material lifespan	Limited by light absorption efficiency	High cofactor costs impact overall efficiency
CO_2 Conversion Rate	High at moderate to high temperatures	Can be high based on applied potential and choice of catalyst	Hampered by poor selectivity and product variety	Less productive, slow reaction rates
Catalyst Durability	Robust; choice of reducible supports enhances durability	Often short lifespan due to rigorous operational conditions	Challenges with catalyst degradation and by-product formation	Enzyme stability and recyclability need enhancement
Capital and Operational Costs	Relatively cost-effective due to higher efficiencies, and easy integration with reforming industries	Relatively high due to the need for optimizing efficiency and current density. Still requires technological maturity for CO_2 conv.	Significant capital investment and energy required, especially for wide bandgap semiconductors	Costly due to the high price of enzymes and cofactors
Technological Maturity	Advanced	Remains limited in industry due to practical challenges	Processes are complex and mechanisms are not fully understood	Requires advancements in enzyme modification and immobilization
Reaction Mechanisms	Complex but widely studied on a variety of catalysts	Complex with limited understanding. Requires intricate tools to monitor reaction intermediates near electrodes in liquid medium	Involves intricate mechanisms that are poorly understood	Constrained by the complexity of biological systems
Selectivity	High and can be tailored for desired outcomes	Low; produces a mix of products. High conversion is often reported with broad product distribution	Often poor due to multiple possible reactions	Can be very selective. Dependent on the specificity of biological pathways
Scalability	Highly scalable and suitable for industrial scale-up	Faces practical challenges in scaling. Requires further technological development.	Limited scalability due to technical and efficiency constraints	Challenging due to the need to maintain microbial cultures and nutrient delivery
Downstream Processing	Simplified due to few by-products	Could require separation of multiple by-products	Complexities in separating the catalyst from the product increase expenses	Demands efficient cofactor regeneration and faces genetic knockout issues
Potential for improvement	Relatively well-established with room for incremental improvements based on catalyst and reactor design	Requires catalysts with fast electron transfer and robust transport features	Needs optimization of photocatalysts and treatment processes	Genetic engineering is suggested but leads to challenges like genetic knockout

Recently, the literature documents the generation of liquid fuels, aromatics, and olefin compounds via the thermal catalytic hydrogenation process applied to CO_2 [12,46,47]. In addition, studies indicate that the inclusion of structured zeolites in thermo-catalytic hydrogenation processes has the potential to enhance the selectivity of hydrocarbon prod-

ucts [48,49]. For example, by integrating a Fe-Zn-Zr catalyst with H-ZSM-5, a notable selectivity for isoalkane products, reaching up to 91.9%, can be achieved [49]. Hence, utilizing the thermal CO_2 hydrogenation approach for zeolites as a catalytic medium brings forth a spectrum of advantages, underscored by their structural features that dictate the pathways of the hydrogenation reaction (more in Section 3.1). In addition, zeolites are highly effective in thermal CO_2 hydrogenation due to their extensive surface area and porosity, which provide numerous active sites, enhancing reaction rates and energy efficiency (more in Section 3.2). Their selective pore structure also plays a crucial role by ensuring molecular sieving, allowing only specific hydrocarbon production, thus increasing selectivity and reducing the need for further separation processes. This makes zeolites exceptionally suitable for controlled and efficient chemical processes. The acidity of zeolites is adjustable, which can be tailored to enhance catalytic activity for thermal CO_2 hydrogenation (more in Section 3.3).

Furthermore, zeolites' thermal stability is also pivotal, as they withstand the necessary high temperatures for thermal hydrogenation, preserving catalytic activity (more in Section 3.4). Additionally, zeolites' ability to be regenerated through thermal treatments allows for their reuse, ensuring economic viability. The ability to regenerate zeolites thermally without significant loss of structural integrity or catalytic activity is a crucial advantage over other catalysts that might degrade or require complex regeneration processes. This is particularly aligned with the characteristics emphasized by the synthesis methods for zeolites; bottom-up and top-down approaches (more in Section 4). This renderability, along potential cost savings and a reduced environmental impact due to less frequent catalyst replacement and decreased waste, positions thermal CO_2 hydrogenation with zeolites as a method that is both efficient and sustainable compared to the aforementioned hydrogenation approaches. Furthermore, zeolites are already widely used in various industrial applications, including oil refining and petrochemical processes [50]. Thus, their use in CO_2 hydrogenation does not require radically new technologies or setups. This compatibility with existing industrial infrastructure and processes reduces the barriers to implementation and capital investment, making it a more feasible option compared to other methods that might require specialized equipment or conditions.

3. Influential Parameters

Zeolites, with their tunable structural and functional properties, are key catalysts in CO_2 hydrogenation processes [51,52]. These structured zeolites offer specific pore structures, a balanced density of acid/basic sites, and the capacity to support and stabilize active metal sites, making them essential for controlled catalytic activity and improved product selectivity. This section explores complex parameters influencing zeolite performance in CO_2 hydrogenation, such as their composition, bimodal mesoporosity, oxygen vacancies, Si/Al ratio, thermal stability, structural integrity, and electrical and plasma interactions. Understanding these factors is crucial not only for defining their role in developing effective and sustainable processes for converting CO_2 into valuable chemicals but also for optimizing zeolites for their potential in industrial applications. Selected examples are presented further to highlight this key aspect of structured zeolites in CO_2 conversion.

3.1. Interplay of Composition and Preparation

Structured zeolites, typically modified with metal-based catalysts, present a multifaceted platform where the interplay between the zeolite topology, metal characteristics, and preparation methods determines the efficiency and outcome of the hydrogenation process. Metal-based catalysts are instrumental in defining product selectivity. These catalysts, when integrated with zeolites, leverage the unique hybrid nature of active sites within the zeolite framework. This configuration supports specific reaction intermediates that dictate the pathways of the hydrogenation reaction, thereby influencing the selectivity toward different hydrocarbons [5]. Wei et al.'s [53] investigation found that the topology of various zeolites, including H-Y and H-BEA, influenced the distribution of hydrocarbons

during fuel production, although CO_2 conversion rates remained consistent. Zeolites with ten-membered rings, such as HZSM-5, were notably efficient in enhancing the selectivity towards larger hydrocarbon molecules in the gasoline range (C_5–C_{11}), with HZSM-5 demonstrating a preference for heavier fractions. Acidity levels were critical, with medium acidity in HZSM-5 (160) favoring the desired reaction, whereas stronger acidity prompted excessive cracking of larger hydrocarbons. Popova et al. [54] developed both mono- and bimetallic catalysts with Ni and Ru on ZSM-5 zeolites, noting the impact of nickel (Ni) content and the introduction of ruthenium (Ru) on their properties. Characterization techniques (XRD, TPR-TGA, TEM, XPS) revealed a fine dispersion of Ni and ruthenium oxide (e.g., RuO_2, RuO_4) across the zeolite's surface and pores (more in Section 5). Tests in CO_2 hydrogenation showed that the 10Ni5RuZSM-5 variant exhibited excellent methane production efficiency, achieving 100% conversion with complete selectivity at 400 °C, and displayed promising stability for practical use. Furthermore, the composition of zeolites, particularly when doped with metals such as lithium (Li), can significantly alter catalyst reactivity. For instance, Kitamura et al. [55] investigated CO_2 hydrogenation using Rh zeolites enhanced with Li (see Figure 3a,b). They found that increasing Li levels shifted the primary product from methane to CO and ethanol, with a notable increase in ethanol production when CO was present. FTIR and TPR analyses suggested that Li additives fostered new reaction pathways on the catalyst surface, leading to improved CO_2 adsorption and stabilization of adsorbed CO species. Similarly, incorporating molecules like Na^+, N, and Ge into the ZSM-5 zeolite framework was demonstrated to lower the energy barriers for CO_2 hydrogenation, thereby enhancing the overall catalytic efficacy [56].

Preparative methods also significantly contribute to tuning the characteristics of zeolites for the best performance in CO_2 hydrogenation. The synthesis method of zeolite, such as the choice of template, calcination conditions, and metal loading approaches, can also significantly affect the structural and chemical properties of the catalyst. Liu et al. [57] investigated how alkali metal promotion in Co-zeolite catalysts affects product selectivity, comparing IWI with the IE approach (see Figure 3c,d). Their findings revealed distinct differences: IWI led to a higher yield of olefins and C_{5+} hydrocarbons, attributed to an elevated Si/Al ratio (see Figure 3e). In contrast, the IE method's selectivity remained largely unaffected by changes in the Si/Al ratio, likely due to alkaline poisoning (see Figure 3f). Hence, the zeolite framework topology determines the behavior of CO_2 and hydrogen (H_2) in the active sites. Specific zeolite structures with specific synthesis procedures can selectively adsorb these reactants and promote their transformation into the desired products under the appropriate conditions. For instance, Ramirez et al. [58] explored the significant role of zeolite topology in the direct conversion of CO_2 into valuable hydrocarbons. They reported that catalysts using different zeolite frameworks, specifically MOR and ZSM-5, exhibit markedly different behaviors in their ability to convert CO_2 to olefins and aromatics, respectively. The study also highlighted that the unique structural characteristics of MOR favor olefin production, while the properties of ZSM-5 enhance aromatic synthesis under the same reaction conditions. This variation is attributed to how these zeolite structures interact with potassium superoxide-doped iron oxide catalysts, influencing the formation of surface formate species and the activity of carbocation intermediates (see Figure 4).
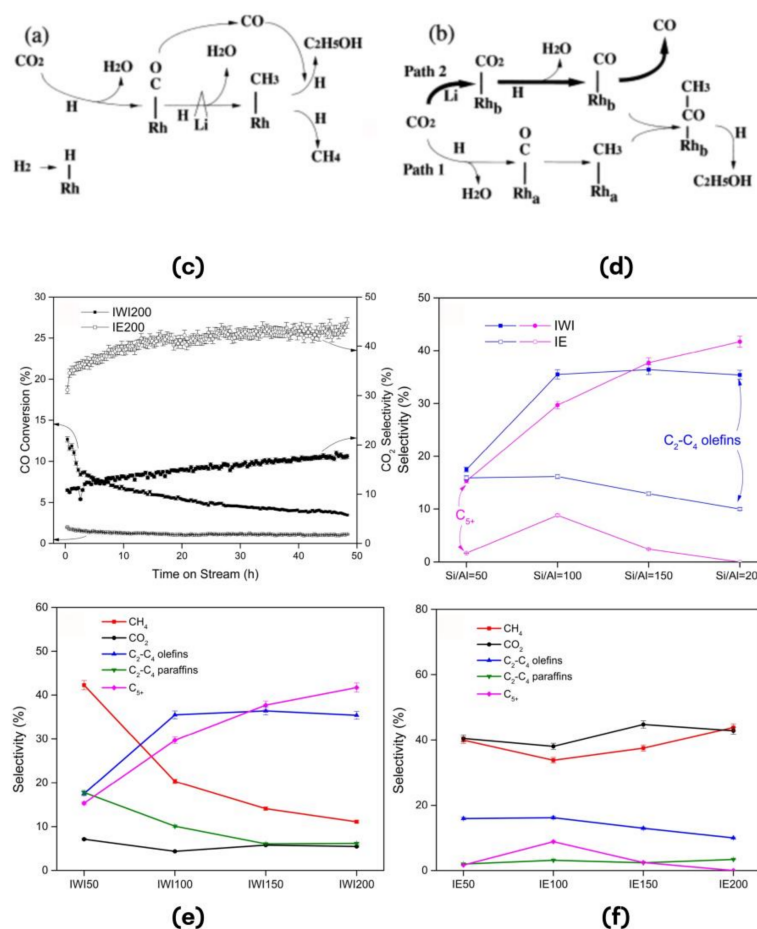
Figure 3. (**a**,**b**) Visual representation of the chemical interactions and mechanisms on a Li/RhY catalyst consisted of 5 wt% Rh and a Li/Rh ratio of 10 [55]. (**c**,**d**) Analysis of the impact of preparative techniques, specifically incipient wetness impregnation (IWI) and ion exchange (IE), on the performance of Co-zeolite catalysts [57], focusing on (**e**) product selectivity for IWI catalysts at different Si/Al ratios and (**f**) product selectivity for IE catalysts at varying Si/Al ratios.
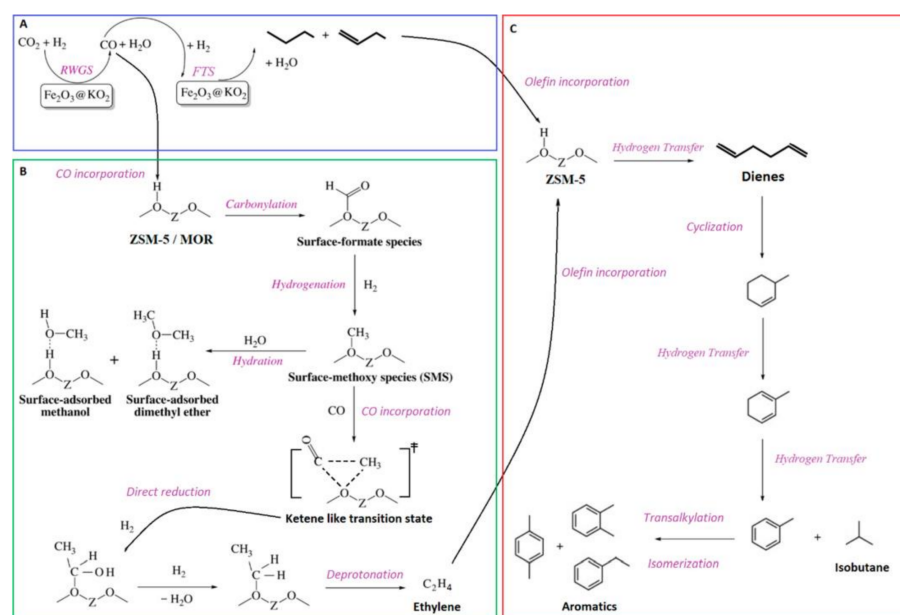

Figure 4. Suggested CO_2 conversion pathways to produce light olefins and aromatics [58]. (**A**) pathway for utilizing only Fe_2O_3@KO_2/zeolite catalyst (**B**) CO integration pathway on MOR and ZSM-5

(**C**) Aromatics generation pathway on ZSM-5. ‡ indicates the formation of a short-lived intermediate in the reaction pathway. Specifically, it points to a "ketene-like transition state" during CO incorporation into a surface-adsorbed dimethyl ether.

3.2. Bimodal Mesoporous Structure and Surface Oxygen Vacancies

Bimodal mesoporous zeolites, with their dual-sized pores, optimize CO_2 hydrogenation by boosting mass transfer and catalytic site availability. The adjustment of the zeolite's pore architecture can be accomplished by developing a hierarchical pore system. This system ensures that the zeolite not only retains its intrinsic micropores but also incorporates supplementary meso- or macropores, which may be located either within or between the crystals [59,60]. In this way, the mesopores enhance the ingress of reactants like CO_2 and H_2, while surface oxygen vacancies act as active sites or alter adjacent metal sites to better activate CO_2 and promote essential reduction steps in the hydrogenation process. Song et al. [61] explored the influence of zeolite morphology and pore structure, focusing on aromatics production using a $Cu-Fe_2O_3$-HZSM-5 catalyst. The study involved commercial zeolites and those synthesized via various methods such as dry-gel, hydrothermal, and phase-transfer techniques. Their research found a preference for mesoporous structures in enhancing aromatic production, particularly noting that the HZSM-5 produced by the phase-transfer method showed an improved selectivity for aromatics from 56.61% to 61.94%, attributed to its rich 5–12 nm pores, which facilitate the formation of aromatics like BTX. In the same investigation, they also proposed an "H recycling mechanism" for CO_2 hydrogenation to aromatics, suggesting that hydrogen species from the zeolite can move to the oxide interface and interact with adsorbed CO_2 at oxygen vacancies. Similarly, Tian et al. [62] developed M(Z, Ca, In)-UIO-66/palygorskite-HZSM-5 zeolite tandem catalysts for converting CO_2 directly into aromatics, employing Diffuse Reflectance Infrared Fourier Transform Spectroscopy (DRIFTS) and Density Functional Theory (DFT) to investigate the reaction mechanisms. The standout, 6%Zn-UIO-662/Z5 at 550 °C, achieved the highest specific surface area of 437.50 m^2/g, optimal acidity, and numerous oxygen vacancies, leading to an impressive CO_2 conversion rate and aromatics selectivity of 88.8%.

The adsorption properties and pore size distributions of Zn-UIO-66/Z5 tandem catalysts across varying calcination temperatures and Zn contents are depicted in Figure 5. The catalysts exhibited type IV isotherms with H4-type hysteresis at higher pressures ($P/P0 = 0.7$–1.0), indicating the presence of both micropores and mesopores, the latter attributed to the agglomeration state of acidified palygorskite nanofibers. Adjusting crystallization times during Z5 zeolite preparation allowed for controlled interstitial pore formation between nanofiber crystals, thus improving reactant and product diffusion. Notably, the addition of Zn enhanced the adsorption capacities, with optimal results at 6% Zn inclusion. However, excessive calcination temperatures can compromise structural integrity and reduce adsorption capacities. The integration of Zn and UIO-66 into Z5 zeolite and the presence of acidified palygorskite were key to enhancing pore structure and surface area, which in turn improved the catalyst's performance in CO_2 hydrogenation to aromatics. The pore size distribution is predominantly centered around 10–20 nm, contributing to efficient catalysis. Therefore, the mesoporous structure within zeolites enhances the movement of olefin intermediates towards acidic sites. This improved diffusion pathway leads to increased production yields of aromatic compounds. Furthermore, in the work by Yan et al. [63], they discovered that Ni catalysts supported on zeolites with lower Si/Al ratios (such as 4A, Ni-5A, and Ni-13X) possess large Ni nanoparticles that engage weakly with the support and exhibit lower activation temperatures, leading to notable CO_2 methanation activity, with conversions between 70.4–70.9% and a high methane selectivity of 92.4–96.4%. In contrast, zeolites with higher Si/Al ratios and mesoporous structures (such as Ni-ZSM-5 and Ni-BEA), while demonstrating smaller Ni particles and stronger metal-support interaction, resulted in lower CO_2 conversion rates (71.2–73.4%) and methane selectivity, indicating another crucial role of mesopores in catalytic performance. When selectivity decreases in conjunction with

the mesoporous structure of zeolites, it suggests that while the mesopores may enhance the accessibility of reactants to the catalytic sites by improving diffusion, they may also allow for a wider range of reactions to occur, which can lead to a broader array of products. In other words, the larger mesopores are not as selective in facilitating only the desired reaction pathways; instead, they might enable side reactions, leading to an assortment of products rather than selectively yielding the target molecule. For CO_2 hydrogenation specifically, if a mesoporous zeolite results in decreased selectivity, it means that while more CO_2 might be converted (enhanced activity), the proportion of the desired product (such as methane in the case of methanation in Yan et al.'s study [63]) is lower because other products are also formed. This could be because mesopores allow not only the desired reactants to access the active sites more easily but also potentially allow unwanted reactants to participate in the reactions, or they might not effectively stabilize the transition states leading to the desired products. Overall, while bimodal mesoporosity and surface oxygen vacancies can improve catalytic activity, their influence on selectivity is a delicate balance that requires careful optimization to favor the desired CO_2 hydrogenation pathways.
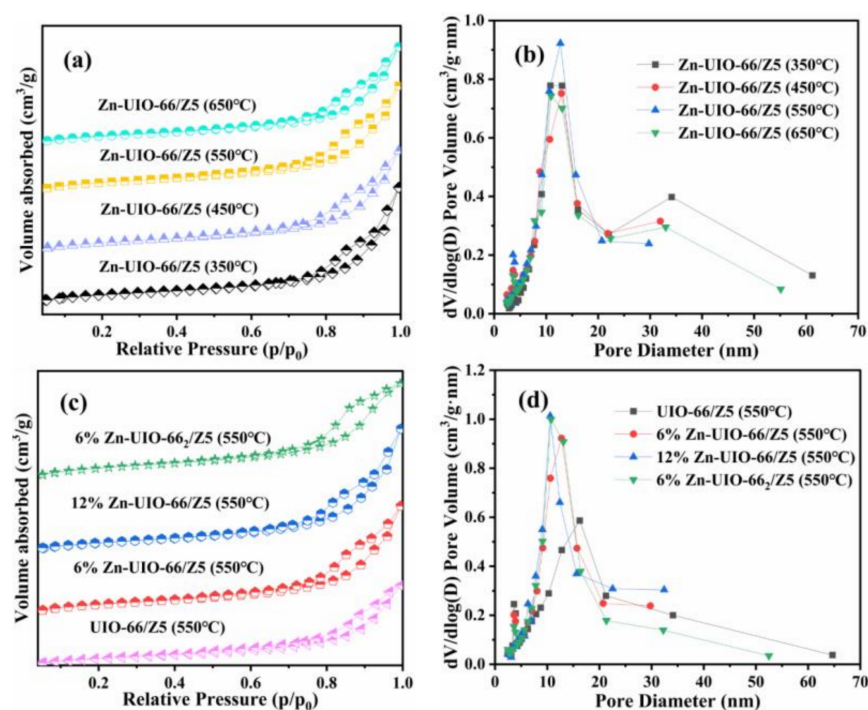

Figure 5. Bimodal mesoporous performance [62]: (**a**) N_2 adsorption–desorption isotherms, and (**b**) pore size distribution for Zn-UIO-66/Z5 at varying calcination temperatures. (**c**) N_2 adsorption–desorption isotherms, and (**d**) pore size distribution for Zn-UIO-66/Z5 with different zinc concentrations.

3.3. Si/Al Ratio

Zeolites with minimal acidity tend to promote hydrogen transfer reactions, often leading to the generation of longer-chain hydrocarbons. In contrast, an excessive number of active sites may be conducive to the formation of saturated hydrocarbons, eventually leading to coking [11]. Thus, the Si/Al ratio must be adjusted with high precision, because this ratio is a direct measure of acidity, to maximize the number of Brønsted acid sites for the best performance. Da Costa-Serra et al. [64] found that Ni-based catalysts mounted on delaminated ITQ-2 zeolite, when presenting higher Si/Al ratios, demonstrated enhanced catalytic activity attributed to increased hydrophobicity. The catalytic outcomes for the ITO-2 and ZSM-5 frameworks varied based on their aluminum content, with high aluminum leading to consistent catalytic behaviors across different zeolite types. Notably, a reduction in aluminum content in the support contributes significantly to catalytic efficiency, as seen in delaminated ITO-2, identified by XRD (see Figure 6a) to have smaller NiO crystallite

sizes, resulting in higher CO_2 conversion (50% improvement) and CH_4 selectivity (98%). However, the size distribution of Ni^0 particles in the 5Ni/ITQ-2(∞) sample remains tightly controlled and closely matches the pre-reaction size, measuring 2.8 nm after the reaction compared to 2.4 nm beforehand (see Figure 6b).
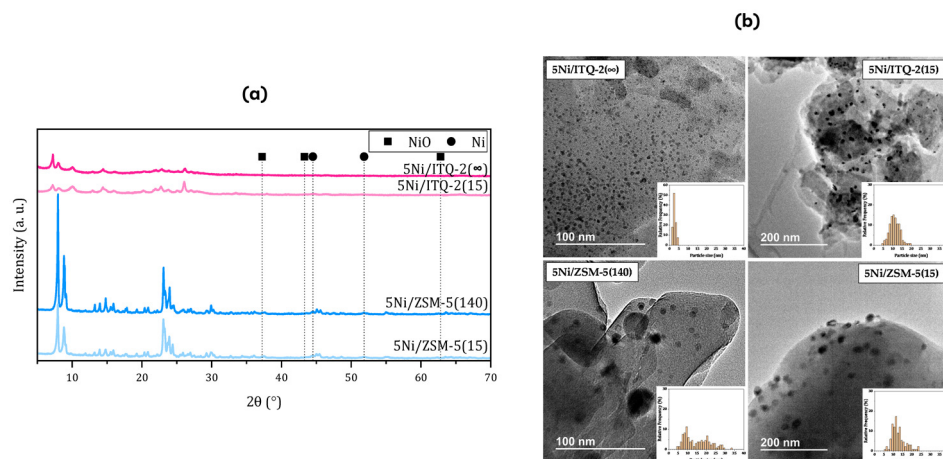

Figure 6. Catalytic Activity of Ni catalysts [64]: (**a**) XRD profiles when mounted on ITQ-2 and ZSM-5. (**b**) HR-TEM image of particle size distribution of Ni^0 in the 5 wt.% Ni catalyst supported on ITQ-2 and ZSM-5 with varying Si/Al ratios following the methanation reaction.

The study by the same authors revealed that higher aluminum content supports (lower Si/Al ratio) yielded similar performances in catalysts due to enhanced Brønsted acidity and hydrophobicity, which are beneficial for reaction progress. Additionally, a high Si/Al ratio improves the dispersion and stability of Ni nanoparticles, influencing their initial dispersion and subsequent thermal redistribution. This relationship highlights the crucial role of aluminum content and Si/Al ratios in determining the properties and effectiveness of these catalysts, which were also previously reported to be significant for methanation processes [65]. Delving deeper, Tada et al. [66] developed multifunctional catalysts, ZnO/ZrO_2, by blending mordenite (MOR) zeolites with varying Si/Al ratios (9, 14, and 104) with ZnO/ZrO_2 and assessed their impact on CO_2 hydrogenation efficiency using a high-pressure flow reactor. Figure 7 illustrates the space-time yield of various hydrocarbons for three different catalysts, namely MOR009, MOR014, and MOR104, over a span of time.
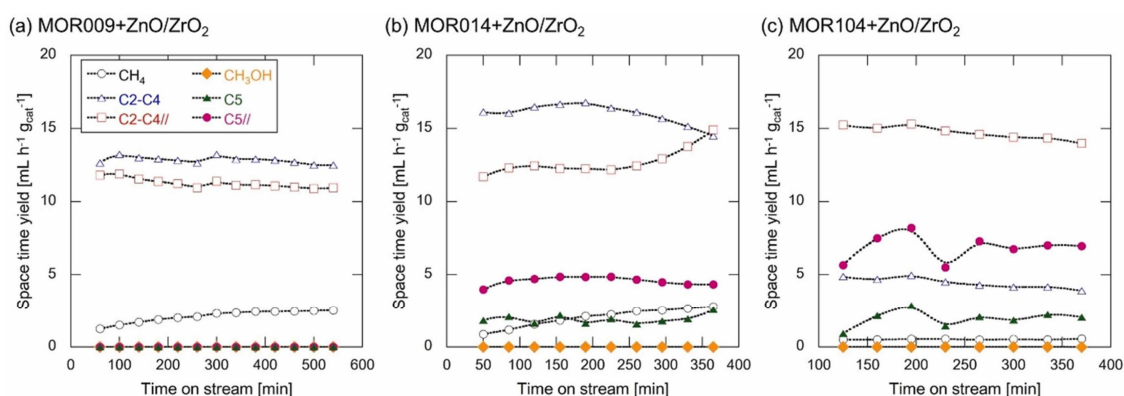

Figure 7. Performance of Zn catalysts supported by MOR zeolites with varied Si/Al ratios and space-time yield of methanol [66]: (**a**) MOR009, (**b**) MOR014, (**c**) MOR104.

For MOR009 (see Figure 7a), the production levels of methane and C_2–C_4 olefins are fairly consistent, though the yield of methanol shows slight fluctuations. Notably, the production of C_5 olefins and paraffins is almost non-existent, which indicates a limited

ability to generate higher carbon number hydrocarbons. In contrast, MOR014 in Figure 7b demonstrates a growing yield of C_5 olefins that peaks midway through the assessment period and then modestly declines, while the output of C_5 paraffins remains stable. This behavior suggests a heightened capacity for creating heavier olefins compared to MOR009. Lastly, the MOR104 catalyst in Figure 7c maintains a stable output of C_5 olefins throughout the period, with only minor fluctuations observed. The production rates for C_2–C_4 paraffins are consistent, although C_5 paraffins exhibit some variability. Overall, MOR104 displays a robust capability for producing C_5 olefins, highlighting its effectiveness for sustained light olefin production. For CO_2 aromatization, Cui et al. [67] assessed the impact of zeolite acidity by varying the Si/Al ratio using a Na-modified spinel oxide ZnFeOx coupled with H-ZSM-5 zeolites. They observed that an increased Si/Al ratio led to a decrease in aromatic selectivity due to the reduced density of Brønsted acid sites, which are pivotal for aromatization. Consequently, a higher density of Brønsted acid sites results in greater selectivity for aromatics [68].

However, greater CO_2 adsorption does not necessarily imply greater hydrogenation activity, which is the main problem with typical zeolite catalysts. The hydrogenation process is not solely dependent upon the amount of CO_2 adsorbed. Instead, it is also dependent upon the availability and reactivity of H_2 within the catalyst system and the catalyst's ability to help the reaction between CO_2 and H_2 to form hydrocarbons. A zeolite with a higher CO_2 adsorption capacity, in consequence of its higher basicity (linked to a lower Si/Al ratio), may be able to retain CO_2 more tightly, thus hindering the reaction with H_2, if the CO_2 is not easily released to react with H_2. The equilibrium between the strength of the adsorption and the reactivity is fragile, whereby strong adsorption could interfere with the catalytic process, while weak adsorption might not capture CO_2 efficiently enough for the reaction. Therefore, the ideal scenario for enhanced hydrogenation activity is not just high CO_2 adsorption but also an optimal level of adsorption that allows for effective interaction with H_2, leading to the formation of the desired hydrocarbon products.

3.4. Porosity, Thermal Stability, and Structural Integrity

The porosity, thermal stability, and structural integrity of structured zeolites are also pivotal for optimizing CO_2 hydrogenation processes. These factors are integral to the zeolite's ability to adsorb reactants, withstand high temperatures, and maintain its structure under reaction conditions, which, in turn, affects catalytic performance, product selectivity, and potentially its commercial applicability. In a pioneering study by Xiang et al. [69], an AFX-type SAPO-56 zeolite was innovatively augmented with copper (Cu) nanoparticles, crafting a multifaceted catalyst aimed at converting CO_2 to methanol. This novel catalyst achieved a CO_2 to methanol conversion rate of 16.4% and showcased an impressive 80.9% selectivity for methanol production. In this study, the strategic dispersion of Cu nanoparticles across the extensive pore network of the SAPO-56 zeolite markedly boosted H_2 adsorption and its subsequent dissociation, facilitating widespread H_2 atom availability. These atoms interacted with the zeolite's intrinsic Lewis acid sites, effectively catalyzing methanol synthesis. The catalyst's hierarchically structured porosity was pivotal in steering product selectivity while ensuring exceptional stability, highlighting its potential for industrial deployment in CO_2 reduction initiatives. Similarly, Cui et al. [70] made significant strides in the catalytic conversion of CO_2 to methanol by creating a zeolite-encapsulated Cu/ZnOx@Na-ZSM-5 catalyst with a core–shell structure derived from bimetallic CuZn-HKUST-1 nanoparticles via hydrothermal synthesis. This design also effectively prevented Cu sintering and enhanced the catalyst's thermal stability. The zeolite framework not only contributes to a higher methanol yield by ensuring a synergistic effect and intimate interaction of the encapsulated nanoparticles but also upholds the structural integrity of the catalyst, promoting sustained activity over prolonged durations. These innovations demonstrate the critical role of porosity and the architectural solidity of zeolites in fostering stable and efficient CO_2 hydrogenation processes.

3.5. Electrical and Plasma Interactions

The control of electrical and plasma properties in catalyst design is also essential for achieving high CO_2 conversion rates and selectivity to the desired products operating under various operational conditions. Figure 8 illustrates a setup for plasma-assisted CO_2 hydrogenation using a dielectric barrier discharge (DBD) reactor [71]. Feliz et. al. [72] observed that zeolite structures affect the ionic conductivity and dielectric constant of the catalyst in plasma-assisted reactions. Lower ionic conductivity facilitates a better CO_2 conversion (34%) because of decreased plasma density and CO_2 dissociation at ambient pressure and temperatures under 100 °C. Owing to zeolites' unique structures, they have been recognized as prospective catalyst supports for DBD plasma systems intended for CO_2-to-methane conversion. Attention has been especially given to Ni-based catalysts within these plasma systems [73,74]. For example, the utilization of Ni/beta zeolite catalysts has been associated with a greater selectivity for methane production, with up to 95% conversion for either CO or CO_2 [75]. It was noted that Ni particles could be redistributed under DBD plasma exposure, which might improve the catalytic process. In addition, this treatment was recommended to promote the desorption of the adsorbed molecules from the catalyst, whereby these adsorbed molecules have much weaker bonds compared to their gaseous counterparts. Reactive species that were produced by plasma were believed to play a role in removing the adsorbed CO molecules, which is a key step for achieving higher methane yield, while the accumulation of water on the catalyst's active sites, emerging as a reaction byproduct, poses a significant limitation for thermal CO_2 methanation by obstructing access to these sites, in line with the insights provided by Sabatier's principle [76,77].
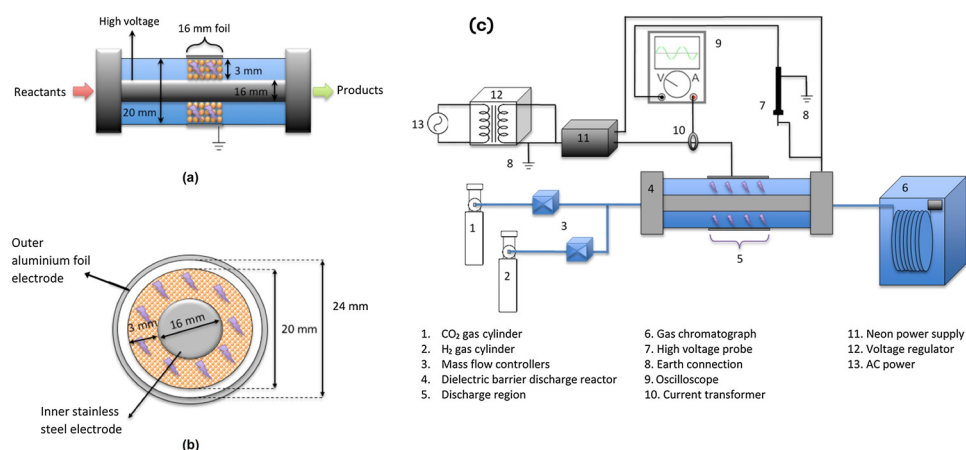

Figure 8. Plasma-assisted catalytic conversion of CO_2 to ethane using a DBD reactor [71]: (**a**) reactor set-up, (**b**) cross-sectional view of the reactor, (**c**) process flow diagram of the overall set-up.

When discussing electrical and plasma interactions in such catalytic systems, it is useful to look at the wider meaning of ionic conductivity and its impact on catalytic processes. The work of Henckel et al. [78] is a relevant example of this, as they used Electrochemical Impedance Spectroscopy (EIS) to investigate the interaction between the catalyst and ionomer, with a particular interest in the transport of hydroxide ions in the electrochemical CO to ethylene conversion. The results confirmed that fine-tuning ionic conductivity can substantially promote the Faradaic efficiency of ethylene and the cell voltage. Although the study did not directly concern zeolite materials and hydrogenation of CO_2, the principles that can be derived from their work are of great interest to CO_2 hydrogenation over structured zeolites. The principle of modulating ionic behavior to maximize catalyst performance is a general concept that is observed in diverse catalyst systems, including zeolites for CO_2 hydrogenation. As it happens in electrochemical systems where both ionic transport and electrical interactions are crucial for the reaction outcomes, in zeolite catalysts, these characteristics can affect the diffusion of reactants and

the distribution of active sites and subsequently determine the efficiency and selectivity of the hydrogenation reactions.

4. Synthesis Methods

Structured zeolites can be synthesized in many ways by utilizing precursors in soluble form and reducing them, or by using existing solid compounds and modifying their structures. These methods can be broadly grouped into two categories: bottom-up and top-down approaches [79], as shown in Figure 9a.
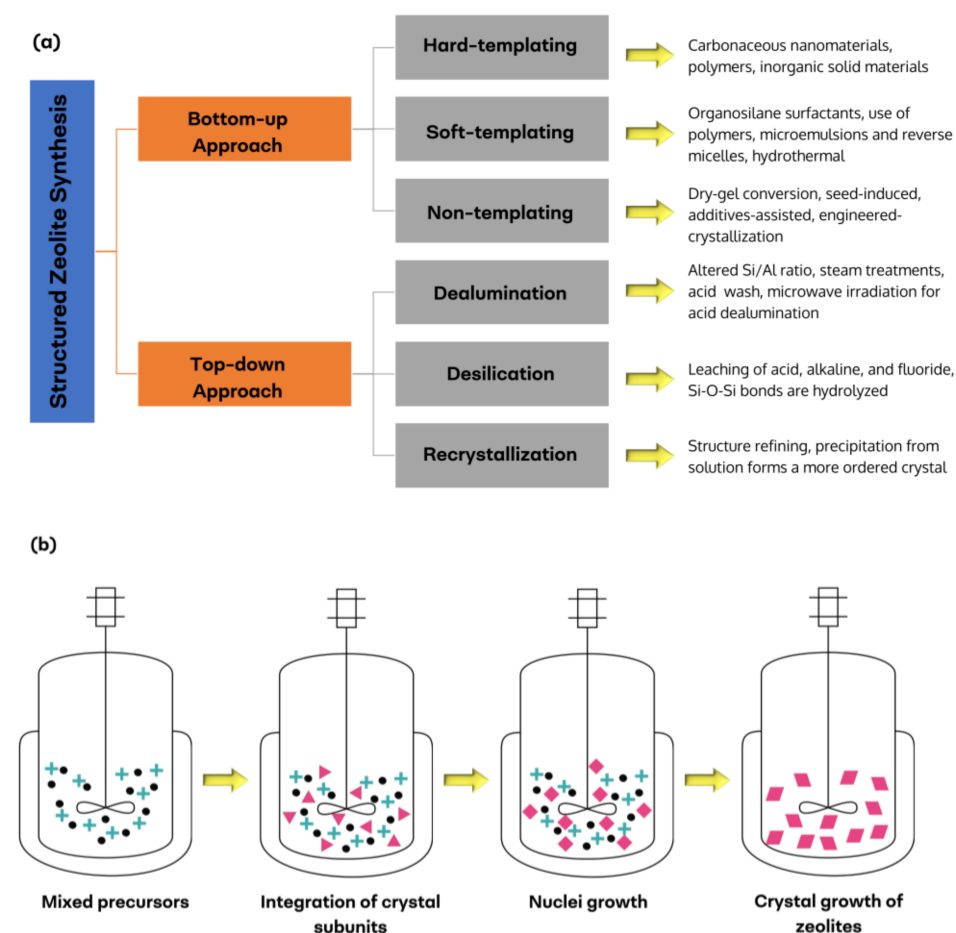

Figure 9. Pathways for zeolite synthesis. (**a**) Conventional routes and their preparation principles. (**b**) Schematic formation of new crystalline phases via hydrothermal synthesis.

4.1. Bottom-Up Approach

The bottom-up approach focuses on creating mesopores within the zeolite structure using a variety of templating methods. Hard-templating involves using rigid carbonaceous materials like carbon black, carbon nanotubes/nanofibers, or 3DOM carbon templates to shape the forming zeolite structure [80–82]. In a study by Wu et al. [83], Ni nanoparticles were encapsulated within microporous graphene-like carbon derived from a NaY zeolite template. The resulting Ni-loaded catalyst demonstrated efficient CO_2 hydrogenation to methane, with 50% conversion and 96% methane selectivity at high space-time yields, showcasing remarkable long-term stability. Subsequently, soft-templating is less rigid and facilitates the crystallization of zeolites by forming interactions with zeolite precursors or frameworks through a range of covalent and electrostatic forces, including van der Waals interactions, hydrogen bonds, and ionic attractions [84]. It utilizes quaternary ammonium surfactants such as cetyltrimethylammonium bromide (CTAB) or cationic polyelectrolytes such as polydiallyldimethylammonium chloride (PDDA-Cl) and polydiallyldimethylam-

monium chloride (PDADMAC) [85–87]. These create microporous zeolite crystallization, while the organosilane's hydrophobic alkyl chains direct mesopore formation [88]. However, the conventional hydrothermal synthesis method (see Figure 9b), is notable for its substantial byproduct generation, including waste materials and gases such as CO_2 and N_2, and its prolonged crystallization process typically leads to reduced production efficiency [89]. Therefore, alternative 'green' synthesis routes have been sustainably employed to overcome such concerns. For example, Tian et al. [90] described an innovative approach for crafting SAPO-34 zeolites with layered porosity using only rice husk as the silicon source. The resulting bio-SAPO-34 exhibited high efficiency in converting CO_2 to olefins, with an impressive C_2–C_4 olefin selectivity of 94.5%. The study found that CH_3O^* species were pivotal intermediates, with DRIFTS analysis showing their formation on the ZnZrOx catalyst surface and subsequent transfer to the acid sites of bio-SAPO-34 for effective carbon–carbon coupling. In addition, and interestingly, Din et al. [91] performed the green synthesis of bimetallic catalysts supported on zeolites, whereby it involved the deposition of Cu and Co onto the zeolite rather than the synthesis of the zeolite framework itself, which did not require extensive washing of precipitates. The process included dissolving the metal acetates in water, adding zeolite to the solution, adjusting the pH with sodium hydroxide, and maintaining the mixture at a specified temperature while stirring. The final product was then dried, resulting in the formation of bimetallic Cu-Co/zeolite catalysts. The ideal balance of Cu:Co at a 1:1 ratio was determined to be the most effective among the various metal combinations tested, leading to the highest observed rate of methanol synthesis.

Furthermore, non-templating methods rely on alternative strategies like one-pot synthesis, dry-gel conversion, or seed-induced crystallization without using traditional templates [54,89]. For instance, Wei et al. [53] developed a Na–Fe_3O_4/HZSM-5 catalyst using a one-pot synthesis technique. This catalyst demonstrated the ability to transform CO_2 into hydrocarbons within the gasoline range (C_5–C_{11}), achieving a selectivity of 78% among hydrocarbons and limiting methane to just 4%, with a CO_2 conversion rate of 22% under conditions pertinent to industry. They built the catalyst at the molecular level and relied on chemical reactions between iron salts and NaOH in solution to spontaneously form the catalyst without a structural template.

The bottom-up approach to structured zeolite synthesis is not without difficulties. A principal issue is the intrinsic fragility of hierarchical zeolite structures, which could result in loose intermolecular interactions, thereby affecting mechanical stability and charge transport [92]. This can be an especially serious issue when zeolites are used under the high-temperature and high-pressure conditions characteristic of CO_2 hydrogenation processes. One possible approach is to optimize the strength and performance of the materials by linking the molecules through strong covalent bonding that involves the reaction directly on the surfaces [92]. Furthermore, the bottom-up approach sometimes struggles with the controlled physical and chemical transformations within liquid droplets, a process that is integral to the synthesis of zeolites [93]. An alternative method, encompassing sol-gel and aerosol-assisted approaches, is proposed due to its enhanced focus on controlling the physical and chemical properties during the synthesis of nanomaterials, particularly resultant zeolites [94,95]. Another challenge in the bottom-up synthesis of zeolites is managing intercrystallite diffusion, which can impede reactant and product movement within the crystalline lattice [96]. To address this, an optimal strategy involves enhancing porosity through methods like dealumination, desilication, and recrystallization. These techniques, which now fall under the top-down approach, modify existing zeolite structures to improve molecular accessibility and diffusion pathways.

4.2. Top-Down Approach

The top-down approach involves modifying pre-existing zeolite structures through post-synthesis treatments to enhance their properties, rather than constructing new materials from the ground up. This method focuses on altering existing materials to develop structures with novel characteristics. Top-down approaches play a vital role in the de-

velopment of hierarchical zeolite structures, which boast improved catalytic properties due to increased surface area and pore volume, as well as the surface properties of the zeolites. Dealumination is a process where aluminum atoms are removed from the zeolite framework through methods such as acid leaching or steam treatment, impacting the Si/Al ratio [97–99]. Its counterpart, desilication, involves the removal of silica atoms, typically by treating them with a base solution [100]. This procedure enhances mesoporosity within the zeolite structure [101]. Recrystallization typically involves dissolving the zeolite in a suitable solvent and then causing the material to precipitate out of the solution, forming a more ordered crystalline structure [102,103]. The parameters of the process, such as temperature, concentration, and choice of solvent, can significantly influence the outcome [89]. For example, Oishi et al. [48] employed a multi-top-down approach to modify MOR zeolite, initially transforming it into a slurry via milling and subsequently recrystallizing it under heat in an autoclave, resulting in nanosized MOR particles. The processed MOR underwent ion exchange with NH_4Cl, fine-tuning its ionic makeup. They then performed dealumination, using different sulfuric acid concentrations to adjust the Si/Al ratio, thus tailoring the zeolite's acidity and enhancing its catalytic abilities. Lastly, defect healing with a fluoride solution was conducted on the dealuminated MOR to mend structural imperfections, optimizing the material. Following the modifications, the enhanced MOR sample exhibited improved catalysis in CO_2 hydrogenation to lower olefins, notably doubling the olefin-to-paraffin ratio from 0.69 to 1.4, thus signifying a more selective and efficient reaction. Furthermore, Liu et al. [57] demonstrated alternative top-down approaches such as incipient wetness impregnation (IWI) and ion exchange (IE) for a series of Co/ZSM-5 catalysts to facilitate CO_2 hydrogenation to value-added chemicals via the modified-FTS pathway. They found that the selectivity for CO_2 hydrogenation on catalysts prepared by IWI strongly depends on the Si/Al ratio. In contrast, such a ratio has little impact on catalysts produced via IE. Enhancing the Si/Al ratio in impregnated catalysts usually improves olefin production, which is associated with acidic features and cobalt reducibility. However, in the same study, altering the Si/Al ratio in ion-exchanged catalysts did not influence the acid properties of K-ZSM-5 for catalytic performance. This lack of effect can be attributed to the introduction of alkali metals, which increased the number of basic sites and reduced the crystallinity. Therefore, it is essential to avoid excessive modification of atoms, as this can lead to the destruction of the crystal structure, thus underscoring the necessity for controlled and balanced treatment processes [50].

The top-down methodology for synthesizing zeolites also encapsulates a set of distinctive challenges that command innovative solutions to further enhance their catalytic performance. Firstly, inadequate characterization methods used for zeolites synthesized by the top-down approach prove to be one of the serious limitations whereby it is crucial to disclose the specific T-sites where the metal centers are situated, as these locations dictate the geometry of the active centers within the zeolites and, consequently, define their reactivity [104,105]. To address this challenge, Dapsens et al. [106] emphasized the utilization of advanced X-ray Absorption Spectroscopy methods, such as the integration of Extended X-ray Absorption Fine Structure (EXAFS) and X-ray Absorption Near Edge Structure (XANES), in overcoming analytical limitations. These techniques were pivotal in the studies conducted by Liu et al. [57] and Ding et al. [107], which focused on the characterization of Co/ZSM-5 and Cu@NaBeta catalysts, respectively. Their investigations demonstrated that the synergistic interaction between metal nanoparticles and the zeolitic framework plays a critical role in forming high-performance catalysts for CO_2 hydrogenation to olefins and ethanol accordingly. Next, the structural integrity of catalysts can be compromised by water generated during reactions. Specifically, during a CO_2 methanation reaction, zeolites are vulnerable to dealumination, a process in which aluminum atoms are stripped from the framework. This occurs under high operating temperatures and pressures in the equipment, particularly in the presence of water molecules, leading to partial degradation or impairment of the zeolite structure [108]. Such conditions can also result in the clogging of the zeolite pores as the released aluminum accumulates within

the structure, further compromising its effectiveness. To mitigate these concerns, Bacariza et al. [109] suggested that commercial USY zeolites, typically used in fluid catalytic cracking (FCC) industrial processes and subjected to ultra-stabilization treatments including controlled steaming for dealumination, could serve as effective supports for CO_2 methanation catalysts. The same authors also pointed out that employing USY zeolite as a support demonstrated promising results, with no structural damage observed in the samples after both conventional and deactivation tests, even when exposed to water during the reaction. In addition, Verboekend et al. noted desilication issues like limited Si/Al ratio control, over-extraction of silicon, structural damage, ineffective pore agents, and uneven mesopores affecting zeolite performance [110]. Optimizing zeolite desilication involves careful control of alkali treatment conditions and the use of pore-directing agents to ensure consistent pore size while maintaining the zeolite's structure and acid sites [111]. Selective treatment is key to achieving ideal mesoporosity without compromising catalytic efficiency. Using tetrapropylammonium hydroxide (TPAOH) for selective desilication, for example, Dai et al. [112] engineered silicalite-1 with precise mesoporosity, achieving nanocube sizes up to 600 nm. This approach also improved CO_2–hydrocarbon conversion, with a marked increase in C_{5+} hydrocarbon selectivity when iron-based catalysts were supported on these tailored zeolites. Similarly, Sharma et al. [113] designed a novel two-bed catalytic system for CO_2 hydrogenation via the MTH pathway, leveraging a desilicated HZSM-5 zeolite to boost hydrocarbon yields, with a notable hydrocarbon selectivity of up to 71.2%. This system, through selective desilication, enhanced the production of longer-chain liquid hydrocarbons, impressively improving C_8–C_{12} selectivity from 29.2% to 42.4%. Finally, recrystallization concerns are not singled out because they can be part of a broader set of synthesis conditions that also include dealumination and desilication. Overall, these conditions collectively impact the structural and compositional modifications of zeolites during the top-down approach.

5. Characterization Techniques

From the preceding sections, it is clear that catalyst characterization techniques are indispensable tools for gaining a comprehensive understanding of the catalytic mechanisms, performance, and intricate behavior of zeolites in catalysis, such as CO_2 hydrogenation processes. These advanced techniques in Table 3 help elucidate the structural and chemical properties of catalysts, which are critical for optimizing their activity and stability under tailored reaction conditions. In this section, we will delve deeper into the specific methods and their applications in detailing the structural adaptations and chemical dynamics of zeolites, which facilitate their efficacy in CO_2 hydrogenation. We will explore how these characterization methods contribute to a better understanding of the interaction between catalysts and reactants and how this knowledge can lead to the development of more efficient catalytic systems. For the subsequent discussions, we will only highlight specific characterization methods from each category, providing detailed illustrations of how these techniques are applied to enhance our understanding of zeolite catalysis in CO_2 hydrogenation.

Table 3. Advanced characterization techniques for structured zeolites in catalytic reactions like CO_2 hydrogenation.

Category	Method	Application
Molecular and Chemical Structure Analysis [5,114,115]	Fourier-transform infrared (FTIR) spectroscopy	Quantify absorption spectra in chemical bonds and functional groups in molecules
	Raman spectroscopy	Postulate information about molecular vibrations, crystal structures, and phase transitions
	Nuclear Magnetic Resonance (NMR) spectroscopy	Provide detailed information on the framework aluminum distribution and the nature of acid sites
	Small-angle X-ray Scattering (SAXS)	Analyze the structural details of materials at the nanoscale level by detecting inhomogeneities and phase separation within

Table 3. *Cont.*

Category	Method	Application
Crystallographic and Phase Analysis [54,115,116]	X-ray diffraction (XRD)	Assess crystalline structures, crystal phases, and crystal defects
	Powder X-ray Diffraction (PXRD)	Analyze powdered crystalline materials for crystal structure identification
	Selected Area Electron Diffraction (SAED)	Obtain crystallographic information from a sample area
Surface and Elemental Analysis [91,117,118]	X-ray photoelectron spectroscopy (XPS)	Examine the chemistry of the surface, including aspects such as elemental composition, chemical and empirical states, and the electronic state of elements
	X-ray Absorption Spectroscopy (XAS)	Determine local geometric/electronic structural order
	Auger Electron Spectroscopy (AES)	Detect emitted energy of electrons from the catalyst surface
Microscopy and Imaging [115,119]	Scanning Electron Microscopy (SEM) Transmission Electron Microscopy (TEM)	Generate high-resolution images of the surface, internal structure, morphology, and crystallography of nanomaterials
Thermal Analysis [4,5,54,115,120]	Temperature-Programmed Reduction-Thermogravimetric Analysis (TPR-TGA)	TPR: Measure the change in chemical state upon heating TGA: Measure changes in physical and chemical states upon heating
	Temperature-Programmed Desorption (TPD)	Investigate adsorption and desorption behaviors on surface interactions and binding energies
	Temperature-Programmed Oxidation (TPO)	Evaluate oxidation behaviors, particularly in carbonaceous materials, catalyst deactivation investigations
	Temperature-Programmed Reaction (TPRe)	Study reaction kinetics, and catalytic stability under different thermal environments
	Temperature-Programmed Surface Reaction (TPSR)	Focus on surface reactions; mechanisms of surface-mediated reactions
	Temperature-Programmed Reduction/Oxidation (TPR-O)	Explore redox properties for redox reactions
	Temperature Programmed Reduction-Differential Thermogravimetry (TPR-DTG)	Determine the temperatures at which reduction events occur and the quantitative aspects amount of oxygen removed from an oxide
	Temperature-Programmed Ammonia Desorption (TPAD)	Observe ammonia-desorption for acid catalysis

Molecular and chemical structure analysis techniques, such as FTIR and Raman spectroscopy, measure molecular vibrations and identify chemical bonds to reveal the composition of substances. NMR spectroscopy offers a detailed view of atomic-level structure, while SAXS enables the investigation of nanoscale inhomogeneities and phase distribution within materials. In a study by Ramirez et al. [5], NMR spectroscopy provided detailed insights into the selective catalytic roles of various zeolites (MOR, ZSM-22, FER, and ZSM-5) to explore the role of CO at the RWGS reaction phase of the modified-FTS route for CO_2 hydrogenation to alkenes, aromatic compounds, and alkanes. Figure 10a highlights how MOR zeolites are inclined towards producing lighter olefins, whereas ZSM-22 zeolites preferentially lead to heavier olefin production. Additionally, ZSM-5 achieves complete ethylene conversion, while MOR and ZSM-22 exhibit the lowest, with MOR specifically favoring paraffin production when ^{13}CO is absent. However, the introduction of ^{13}CO sees MOR attain the highest conversion rate at around 4%, with ZSM-5 and ZSM-22 at roughly 1% (Figure 10b). Solid-state NMR confirms COs direct incorporation into the zeolite structure (Figure 10c), and a notable carbonyl peak at 177.5 ppm associates with methyl acetate suggests a ketene intermediate in the reaction (Figure 10d). This set of NMR figures paints a comprehensive picture of how each zeolite type uniquely influences the reaction pathway and product distribution.
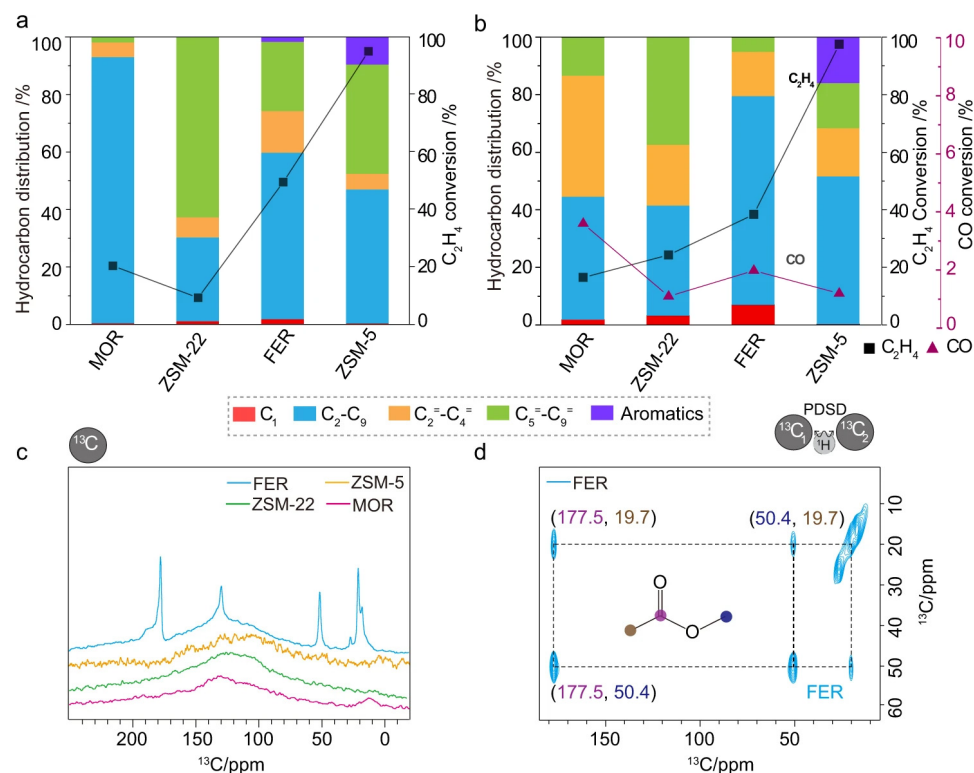
Figure 10. NMR spectroscopic analysis by Ramirez et al. [5] detailed the catalytic activity of various zeolites (e.g., MOR, ZSM-22, FER, ZSM-5), where (**a**) revealed the behavior of these zeolites with ethylene and (**b**) showed the dynamics with enriched ^{13}CO under hydrogen-rich conditions. (**c**) The isotopic enrichment of ^{13}CO correlated with its consumption during the reaction, and (**d**) captured the identification of methyl acetate in FER zeolites, suggesting the involvement of ketene intermediates.

Crystallographic and phase analysis methods encompass techniques like XRD, which examines the arrangement of atoms within crystals and identifies phases and defects. PXRD is tailored to analyze powdered samples for structural identification, while SAED provides crystallographic information from targeted areas within a specimen. On the other hand, microscopy and imaging techniques like SEM and TEM are pivotal for capturing high-resolution images that reveal surface features, internal structures, morphologies, and the crystallography of zeolites. Krachuamram et al. [115] conducted a study to fine-tune the synthesis of NaA/NaX zeolite to maximize surface area and pore volume, finding the best conditions to be a 5 day aging and a 9 h crystallization process in the presence of CTAB and heptane. When used as a support for Ni impregnation at various loadings, the zeolite synthesized under these conditions showed the highest catalytic activity for CO_2 methanation at a 15% Ni level, attributed to the optimal dispersion of Ni on the zeolite surface. Their XRD analyses indicated a notable reduction in the crystallinity of the zeolite, with peak intensities for NaX and NaA decreasing upon Ni impregnation (Figure 11a), and NiO reflections becoming more pronounced. The specific surface area of the zeolite increased significantly from 166.5 m^2/g to 1411 m^2/g with Ni addition (Figure 12b), suggesting a dispersion of Ni that did not disrupt the zeolite's structure, as confirmed by SEM images (Figure 12a). Despite these structural changes, the catalytic efficiency remained primarily reliant on gas adsorption capacities rather than on the surface area, with the presence of Ni-enhancing adsorption sites for H_2 and CO_2 (Figure 11b).

Surface and elemental analysis for zeolites typically employ techniques such as XPS, which analyzes surface chemistry, including elemental composition and states; XAS, for assessing the local structure and electronic state order; and AES, which detects the energies of electrons emitted from surfaces, providing details on the surface's elemental composition. Conversely, under varying thermal conditions, TPR-TGA allows for the study of reduction

processes and zeolite stability. TPD can help determine the strength and nature of adsorption sites by measuring the gases desorbed as the temperature increases. Similarly, TPR-O and TPR-DTG provide insight into the oxidative and reductive characteristics of zeolites, while TPSR and TPAD are employed to examine surface interactions and acidity, respectively.
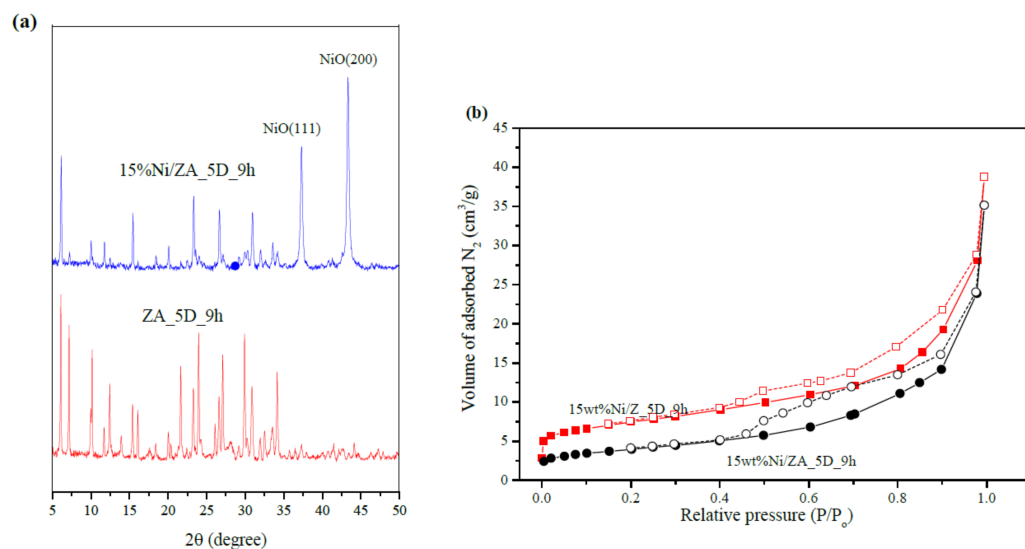

Figure 11. Krachuamram et al. [115] demonstrated the (**a**) XRD profiles of the zeolite framework and the zeolite after 15% nickel has been added. (**b**) Shows the N_2 adsorption–desorption curves for the zeolite treated with an organic phase (Z_5D_9h) compared to the zeolite not treated with an organic phase.
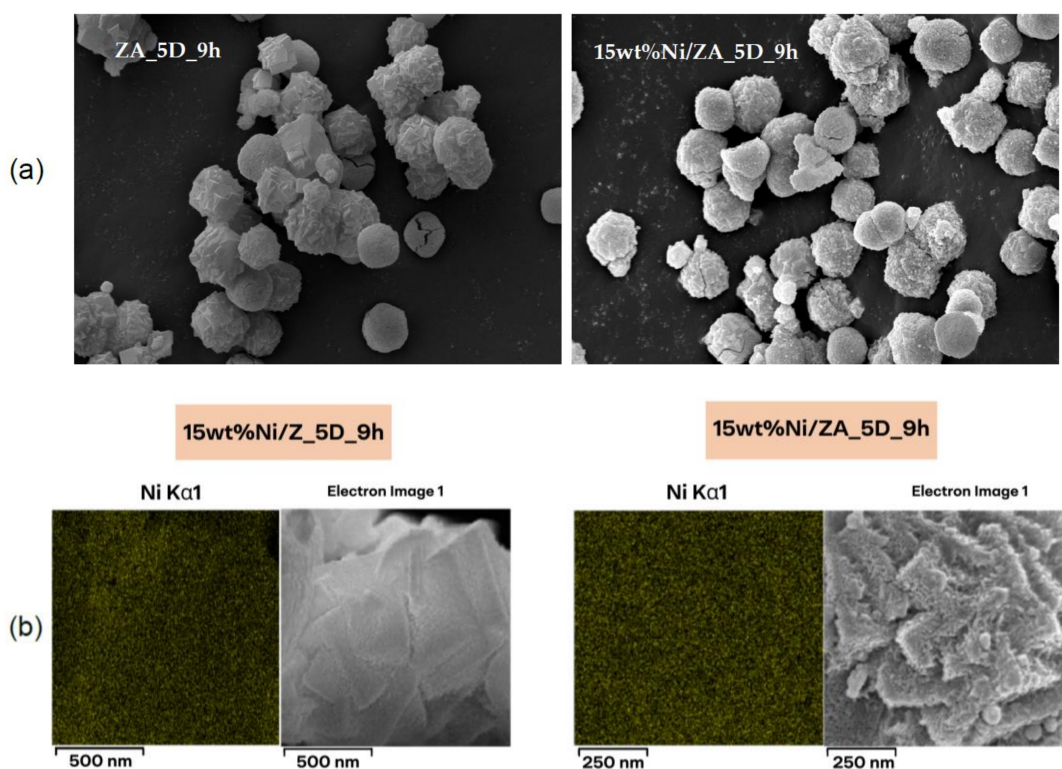

Figure 12. Krachuamram et al. [115] presented (**a**) SEM visuals of the zeolite before and after nickel impregnation and (**b**) SEM images and elemental mapping of the zeolite supports with and without the addition of the organic phase (Z_5D_9h).

Popova et al. [54] developed micro-mesoporous ZSM-5 catalysts modified with Ni and Ru through wet impregnation, examining how Ni content and the addition of Ru

influenced the catalysts' properties by utilizing TPR-DTG to analyze, and they observed distinct reduction peaks. For monometallic samples with 10%Ru, a significant reduction peak occurred at 190 °C, while samples with 5%Ni and 10%Ni exhibited two peaks spanning temperatures of 195–205 °C and 325–360 °C, respectively, suggesting Ni's influence on the reduction process and dispersion on the zeolite (Figure 13a). The XPS analysis post-reduction offered insights into the surface chemistry, indicating a prevalence of RuO_2 for the monometallic samples (e.g., 5RuZSM-5) and a more balanced presence of reduced and oxidized Ru states in the bimetallic samples, such as 10Ni5RuZSM-5 (Figure 13c). These findings aligned with their TPR-DTG results, revealing that bimetallic samples with higher Ni content have more Ni accessible on the surface, which enhanced catalytic activity due to a greater number of active sites, whereby 10Ni5RuZSM-5 exhibits a single, wider peak reaching its apex at 268 °C (Figure 13b). As a result, the 10Ni5RuZSM-5 catalyst showcased high efficiency, achieving 100% selectivity for methane production from CO_2 at 400 °C. This performance, coupled with its stability and the potential for reuse, underscores the catalyst's applicability in practical settings.
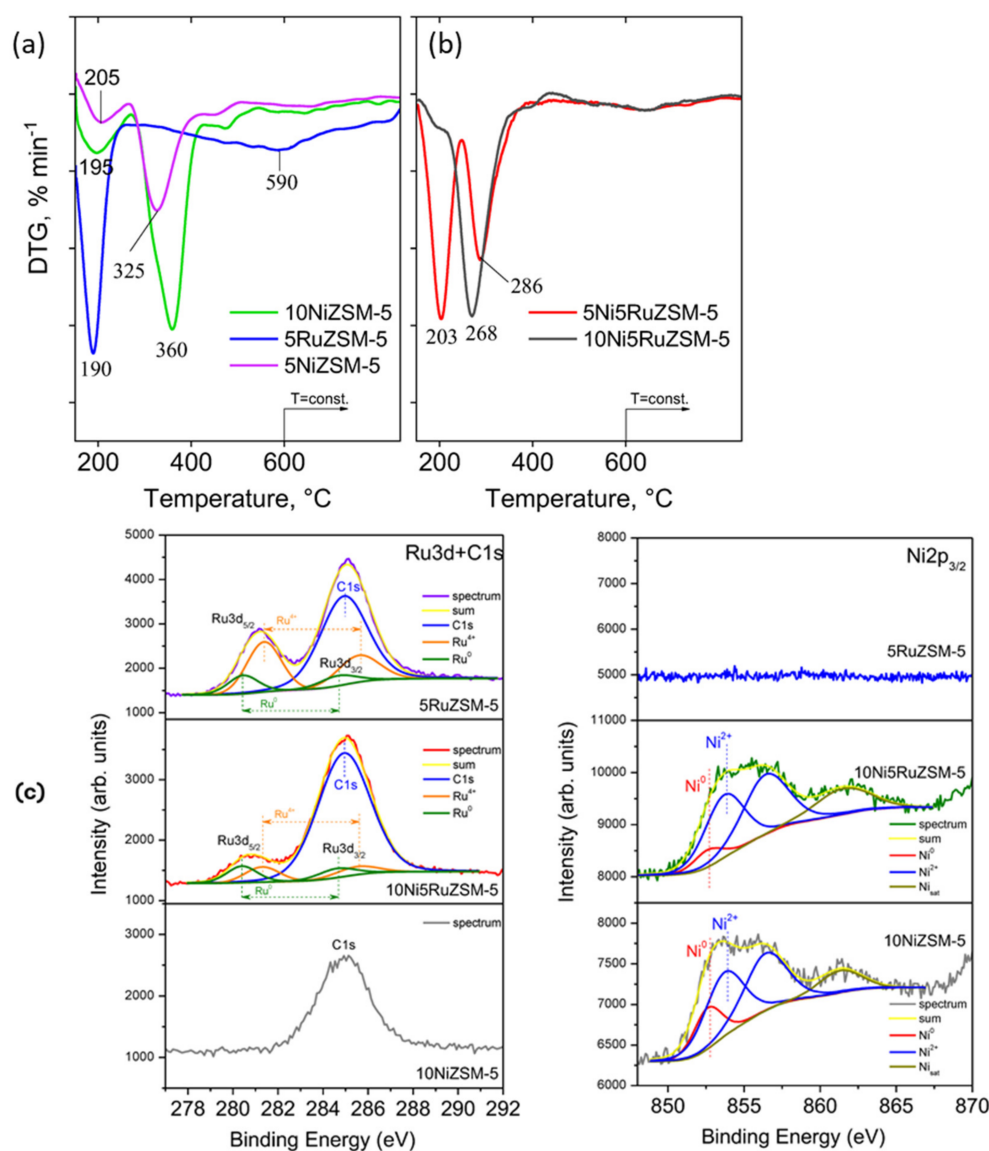

Figure 13. Popova et al. [54] performed TPR-DTG analysis of ZSM-5 zeolites modified with Ni and Ru in (**a**) single-metal and (**b**) dual-metal configurations, and (**c**) XPS profiles for Ru (left) and Ni (right) on the 10NiZSM-5, 5RuZSM-5, and 10Ni5RuZSM-5 zeolites post-reduction.

In common practice, a combination of these characterization techniques in Table 3 often provides a more complete picture. For instance, SEM might be paired with XRD to correlate surface morphology with crystalline structure, or TPR-TGA might be used alongside XPS to evaluate how thermal treatments affect surface chemistry. The choice depends on whether the study aims to optimize the catalyst's structural properties, understand the chemical processes occurring during the reaction, or improve the catalyst's stability and reusability. A multi-technique approach often yields the most comprehensive understanding of the catalytic system.

6. Conclusions

CO_2 hydrogenation over structured zeolites has emerged as a significant technological approach for carbon neutrality, leveraging the conversion of CO_2 into valuable hydrocarbons. Two main methods, the modified-FTS and the MTH route, effectively channel CO_2 into a variety of hydrocarbons, with zeolites playing a pivotal role due to their unique catalytic properties. The thermal hydrogenation method stands out over electrochemical, photocatalytic, biochemical, and chemo-enzymatic approaches for its high efficiency, selectivity, and proven scalability. This positions zeolites as an optimal catalyst for CO_2 hydrogenation, capable of undergoing regeneration and withstanding the high temperatures required for these processes.

Subsequently, the efficacy of structured zeolites in CO_2 hydrogenation depends on the synergy between their composition, preparation, and unique structural properties. Careful calibration of the Si/Al ratio is critical, as it influences acidity and CO_2 adsorption, which are key factors for selectivity and conversion efficiency. Bimodal mesoporous zeolites improve catalytic activity due to enhanced mass transfer and accessible sites but require careful optimization to maintain product specificity. The integration of metals such as Cu and Ni within zeolite frameworks, coupled with plasma treatments, has been shown to boost performance, balancing strong adsorption with necessary reactivity. Attention to electrical and plasma interactions within the catalyst design is therefore paramount, ensuring high conversion rates and desired selectivity in CO_2 hydrogenation processes.

In addition, optimizing zeolite synthesis through bottom-up and top-down methods is critical for enhancing CO_2 hydrogenation. Bottom-up strategies, such as various templating techniques, improve mass transfer by overcoming the diffusion limitations inherent in microporous zeolites and by embedding metals like Cu and Co to augment hydrocarbon production. To combat issues like stability under extreme conditions, these methods are evolving to reinforce molecular bonds and manage intracrystalline diffusion. Top-down methods, including dealumination and recrystallization, further refine zeolite structures, bolstering mesoporosity and catalytic selectivity without altering the crystal integrity. Advanced spectroscopy (e.g., EXAFS and XANES) plays a key role in this fine-tuning, guiding the precise distribution of metal nanoparticles and ensuring optimal catalytic functionality. Furthermore, CO_2 hydrogenation over zeolites benefits from a suite of characterization techniques. FTIR and NMR reveal molecular intricacies and active sites critical for the catalytic process, while phase analyses like XRD detail crystalline structures that influence functionality. Elemental analyses like XPS provide surface analysis crucial for CO_2 interaction, and microscopic imaging like SEM gives insight into morphology and metal distribution, affecting activity and selectivity. Thermal methods, like TPR-TGA gauge stability and reducibility, are essential for catalyst durability.

Looking forward, the trajectory of CO_2 hydrogenation using structured zeolites is set towards transformative progress. Further development of synthesis approaches (bottom-up and top-down), together with sophisticated characterization methods as listed in Table 3, is fundamental for realizing the whole potential of zeolite as an efficient catalyst. With the world moving towards greener and more sustainable options, structured zeolites play a more and more significant role in holistically converting CO_2 into high-value-added chemical products. Achieving optimal selectivity is a delicate balance that is centered on numerous factors, including the accessibility of active sites, metal particle dynamics,

support structure interactions, and overall porosity, each shaped by synthesis and characterization methods. Future research will focus on overcoming current limitations, as remarked in this review, and innovating to enhance catalyst efficiency and selectivity, thereby contributing to the wider goal of reducing the carbon footprint and addressing climate change.

Conflicts of Interest: The authors declare no conflicts of interests.

References

1. Rafiee, A.; Khalilpour, K.R.; Milani, D.; Panahi, M. Trends in CO_2 conversion and utilization: A review from process systems perspective. *J. Environ. Chem. Eng.* **2018**, *6*, 5771–5794. [CrossRef]
2. North, M.; Styring, P. Perspectives and visions on CO_2 capture and utilisation. *Faraday Discuss.* **2015**, *183*, 489–502. [CrossRef] [PubMed]
3. Huang, C.H.; Tan, C.S. A Review: CO_2 Utilization. *Aerosol Air Qual. Res.* **2014**, *14*, 480–499. [CrossRef]
4. Nezam, I.; Zhou, W.; Gusmão, G.S.; Realff, M.J.; Wang, Y.; Medford, A.J.; Jones, C.W. Direct aromatization of CO_2 via combined CO_2 hydrogenation and zeolite-based acid catalysis. *J. CO2 Util.* **2021**, *45*, 101405. [CrossRef]
5. Ramirez, A.; Gong, X.; Caglayan, M.; Nastase, S.-A.F.; Abou-Hamad, E.; Gevers, L.; Cavallo, L.; Chowdhury, A.D.; Gascon, J. Selectivity descriptors for the direct hydrogenation of CO_2 to hydrocarbons during zeolite-mediated bifunctional catalysis. *Nat. Commun.* **2021**, *12*, 5914. [CrossRef] [PubMed]
6. Murciano, R.; Serra, J.M.; Martínez, A. Direct hydrogenation of CO_2 to aromatics via Fischer-Tropsch route over tandem K-Fe/Al_2O_3+H-ZSM-5 catalysts: Influence of zeolite properties. *Catal. Today* **2023**, *427*, 114404. [CrossRef]
7. Dry, M.E.; Hoogendoorn, J.C. Technology of the Fischer-Tropsch Process. *Catal. Rev.* **1981**, *23*, 265–278. [CrossRef]
8. Ibrahim, I.; Harrigan, F. Qatar's economy: Past, present and future. *QScience Connect.* **2012**, *2012*, 9. [CrossRef]
9. Holm-Larsen, H. CO_2 reforming for large scale methanol plants—An actual case. *Stud. Surf. Sci. Catal* **2001**, *136*, 441–446. [CrossRef]
10. Ye, R.-P.; Ding, J.; Gong, W.; Argyle, M.D.; Zhong, Q.; Wang, Y.; Russell, C.K.; Xu, Z.; Russell, A.G.; Li, Q.; et al. CO_2 hydrogenation to high-value products via heterogeneous catalysis. *Nat. Commun.* **2019**, *10*, 5698. [CrossRef] [PubMed]
11. Ojelade, O.A.; Zaman, S.F. A review on CO_2 hydrogenation to lower olefins: Understanding the structure-property relationships in heterogeneous catalytic systems. *J. CO2 Util.* **2021**, *47*, 101506. [CrossRef]
12. Wang, D.; Xie, Z.; Porosoff, M.D.; Chen, J.G. Recent advances in carbon dioxide hydrogenation to produce olefins and aromatics. *Chem* **2021**, *7*, 2277–2311. [CrossRef]
13. Wang, C.; Li, J.; Sun, X.; Wang, L.; Sun, X. Evaluation of zeolites synthesized from fly ash as potential adsorbents for wastewater containing heavy metals. *J. Environ. Sci.* **2009**, *21*, 127–136. [CrossRef] [PubMed]
14. Melaningtyas, G.S.A.; Krisnandi, Y.K.; Ekananda, R. Synthesis and characterization of NaY zeolite from Bayat natural zeolite: Effect of pH on synthesis. *IOP Conf. Ser. Mater. Sci. Eng.* **2019**, *496*, 012042. [CrossRef]
15. Dimitar, G.; Bogdanov, B.; Angelova, K.; Markovska, I.; Hristov, Y. Synthetic Zeolites—Structure, Clasification, Current Trends in Zeolite Synthesis. International Science Conference. Available online: https://www.researchgate.net/profile/Irena-Markovska-2/publication/322211658_SYNTHETIC_ZEOLITES_-_STRUCTURE_CLASIFICATION_CURRENT_TRENDS_IN_ZEOLITE_SYNTHESIS_REVIEW/links/5a990a4f0f7e9ba4297769ff/SYNTHETIC-ZEOLITES-STRUCTURE-CLASIFICATION-CURRENT-TRENDS-IN-ZEOLITE-SYNTHESIS-REVIEW.pdf (accessed on 12 May 2024).
16. Ruiz, A.Z.; Ban, T.; Calzaferri, G.; Brühwiler, D. Synthesis of Zeolite L. Tuning Size and Morphology. *Monatshefte Fuer Chemie/Chem. Mon.* **2005**, *136*, 77–89. [CrossRef]
17. Sun, Q.; Wang, N.; Yu, J. Advances in Catalytic Applications of Zeolite-Supported Metal Catalysts. *Adv. Mater.* **2021**, *33*, 2104442. [CrossRef]
18. Tran, Y.T.; Lee, J.; Kumar, P.; Kim, K.-H.; Lee, S.S. Natural zeolite and its application in concrete composite production. *Compos. Part B Eng.* **2019**, *165*, 354–364. [CrossRef]
19. Cataldo, E.; Salvi, L.; Paoli, F.; Fucile, M.; Masciandaro, G.; Manzi, D.; Masini, C.M.; Mattii, G.B. Application of Zeolites in Agriculture and Other Potential Uses: A Review. *Agronomy* **2021**, *11*, 1547. [CrossRef]
20. Bacakova, L.; Vandrovcova, M.; Kopova, I.; Jirka, I. Applications of zeolites in biotechnology and medicine—A review. *Biomater. Sci.* **2018**, *6*, 974–989. [CrossRef] [PubMed]

21. Kalló, D. Applications of Natural Zeolites in Water and Wastewater Treatment. *Rev. Miner. Geochem.* **2001**, *45*, 519–550. [CrossRef]

22. Fruijtier-Pölloth, C. The safety of synthetic zeolites used in detergents. *Arch. Toxicol.* **2008**, *83*, 23–35. [CrossRef] [PubMed]

23. Wittcoff, H.A.; Reuben, B.G.; Plotkin, J.S. *Industrial Organic Chemicals*; John Wiley & Sons: Hoboken, NJ, USA, 2012.

24. Overa, S.; Ko, B.H.; Zhao, Y.; Jiao, F. Electrochemical Approaches for CO_2 Conversion to Chemicals: A Journey toward Practical Applications. *Accounts Chem. Res.* **2022**, *55*, 638–648. [CrossRef] [PubMed]

25. Perry, S.C.; Leung, P.-K.; Wang, L.; de León, C.P. Developments on carbon dioxide reduction: Their promise, achievements, and challenges. *Curr. Opin. Electrochem.* **2020**, *20*, 88–98. [CrossRef]

26. Nguyen, T.P.; Nguyen, D.L.T.; Nguyen, V.-H.; Le, T.-H.; Vo, D.-V.N.; Trinh, Q.T.; Bae, S.-R.; Chae, S.Y.; Kim, S.Y.; Van Le, Q. Recent Advances in TiO_2-Based Photocatalysts for Reduction of CO_2 to Fuels. *Nanomaterials* **2020**, *10*, 337. [CrossRef] [PubMed]

27. Shehzad, N.; Tahir, M.; Johari, K.; Murugesan, T.; Hussain, M. A critical review on TiO_2 based photocatalytic CO_2 reduction system: Strategies to improve efficiency. *J. CO2 Util.* **2018**, *26*, 98–122. [CrossRef]

28. Bhatia, S.K.; Bhatia, R.K.; Jeon, J.-M.; Kumar, G.; Yang, Y.-H. Carbon dioxide capture and bioenergy production using biological system—A review. *Renew. Sustain. Energy Rev.* **2019**, *110*, 143–158. [CrossRef]

29. Thakur, I.S.; Kumar, M.; Varjani, S.J.; Wu, Y.; Gnansounou, E.; Ravindran, S. Sequestration and utilization of carbon dioxide by chemical and biological methods for biofuels and biomaterials by chemoautotrophs: Opportunities and challenges. *Bioresour. Technol.* **2018**, *256*, 478–490. [CrossRef] [PubMed]

30. Sharma, T.; Sharma, S.; Kamyab, H.; Kumar, A. Energizing the CO_2 utilization by chemo-enzymatic approaches and potentiality of carbonic anhydrases: A review. *J. Clean. Prod.* **2020**, *247*, 119138. [CrossRef]

31. Ribun, V.; Boichenko, S.; Kale, U. Advances in gas-to-liquid technology for environmentally friendly fuel synthesis: Analytical review of world achievements. *Energy Rep.* **2023**, *9*, 5500–5508. [CrossRef]

32. Boretti, A.; Banik, B.K. Advances in Hydrogen Production from Natural Gas Reforming. *Adv. Energy Sustain. Res.* **2021**, *2*, 2100097. [CrossRef]

33. Atsonios, K.; Panopoulos, K.D.; Kakaras, E. Thermocatalytic CO_2 hydrogenation for methanol and ethanol production: Process improvements. *Int. J. Hydrogen Energy* **2016**, *41*, 792–806. [CrossRef]

34. Do, T.N.; Kim, J. Process development and techno-economic evaluation of methanol production by direct CO_2 hydrogenation using solar-thermal energy. *J. CO2 Util.* **2019**, *33*, 461–472. [CrossRef]

35. Zeng, Y.; Chen, G.; Liu, B.; Zhang, H.; Tu, X. Unraveling Temperature-Dependent Plasma-Catalyzed CO_2 Hydrogenation. *Ind. Eng. Chem. Res.* **2023**, *62*, 19629–19637. [CrossRef] [PubMed]

36. Chatzilias, C.; Martino, E.; Katsaounis, A.; Vayenas, C.G. Electrochemical promotion of CO_2 hydrogenation in a monolithic electrochemically promoted reactor (MEPR). *Appl. Catal. B Environ.* **2021**, *284*, 119695. [CrossRef]

37. Zhu, Q. Developments on CO_2-utilization technologies. *Clean Energy* **2019**, *3*, 85–100. [CrossRef]

38. Jhong, H.; Brushett, F.R.; Kenis, P.J.A. The Effects of Catalyst Layer Deposition Methodology on Electrode Performance. *Adv. Energy Mater.* **2013**, *3*, 589–599. [CrossRef]

39. Kalaitzidou, I.; Makri, M.; Theleritis, D.; Katsaounis, A.; Vayenas, C. Comparative study of the electrochemical promotion of CO_2 hydrogenation on Ru using Na^+, K^+, H^+ and O^{2-} conducting solid electrolytes. *Surf. Sci.* **2016**, *646*, 194–203. [CrossRef]

40. Lo, A.-Y.; Taghipour, F. Review and prospects of microporous zeolite catalysts for CO_2 photoreduction. *Appl. Mater. Today* **2021**, *23*, 101042. [CrossRef]

41. Saravanan, A.; Kumar, P.S.; Vo, D.-V.N.; Jeevanantham, S.; Bhuvaneswari, V.; Narayanan, V.A.; Yaashikaa, P.R.; Swetha, S.; Reshma, B. A comprehensive review on different approaches for CO_2 utilization and conversion pathways. *Chem. Eng. Sci.* **2021**, *236*, 116515. [CrossRef]

42. Kumar, B.; Llorente, M.; Froehlich, J.; Dang, T.; Sathrum, A.; Kubiak, C.P. Photochemical and Photoelectrochemical Reduction of CO_2. *Annu. Rev. Phys. Chem.* **2012**, *63*, 541–569. [CrossRef] [PubMed]

43. Yaashikaa, P.R.; Kumar, P.S.; Varjani, S.J.; Saravanan, A. A review on photochemical, biochemical and electrochemical transformation of CO_2 into value-added products. *J. CO2 Util.* **2019**, *33*, 131–147. [CrossRef]

44. Zhang, Z.; Zhang, X.; Ji, X. Developing and Regenerating Cofactors for Sustainable Enzymatic CO_2 Conversion. *Processes* **2022**, *10*, 230. [CrossRef]

45. Long, N.V.D.; Lee, J.; Koo, K.-K.; Luis, P.; Lee, M. Recent Progress and Novel Applications in Enzymatic Conversion of Carbon Dioxide. *Energies* **2017**, *10*, 473. [CrossRef]

46. Gao, P.; Zhang, L.; Li, S.; Zhou, Z.; Sun, Y. Novel Heterogeneous Catalysts for CO_2 Hydrogenation to Liquid Fuels. *ACS Central Sci.* **2020**, *6*, 1657–1670. [CrossRef] [PubMed]

47. Ojelade, O.A. CO_2 Hydrogenation to Gasoline and Aromatics: Mechanistic and Predictive Insights from DFT, DRIFTS and Machine Learning. *Chempluschem* **2023**, *88*, e202300301. [CrossRef] [PubMed]

48. Oishi, R.; Li, D.; Okazaki, M.; Kinoshita, H.; Ochiai, N.; Yamauchi, N.; Kobayashi, Y.; Wakihara, T.; Okubo, T.; Tada, S.; et al. Precise tuning of the properties of MOR-type zeolite nanoparticles to improve lower olefins selectivity in composite catalysts for CO_2 hydrogenation. *J. CO2 Util.* **2023**, *72*, 102491. [CrossRef]

49. Wang, X.; Yang, G.; Zhang, J.; Song, F.; Wu, Y.; Zhang, T.; Zhang, Q.; Tsubaki, N.; Tan, Y. Macroscopic assembly style of catalysts significantly determining their efficiency for converting CO_2 to gasoline. *Catal. Sci. Technol.* **2019**, *9*, 5401–5412. [CrossRef]

50. Azhari, N.J.; Nurdini, N.; Mardiana, S.; Ilmi, T.; Fajar, A.T.; Makertihartha, I.; Subagjo; Kadja, G.T. Zeolite-based catalyst for direct conversion of CO_2 to C_{2+} hydrocarbon: A review. *J. CO2 Util.* **2022**, *59*, 101969. [CrossRef]

51. Hölderich, W.; Hesse, M.; Näumann, F. Zeolites: Catalysts for Organic Syntheses. *Angew. Chem. Int. Ed.* **1988**, *27*, 226–246. [CrossRef]

52. Yilmaz, B.; Müller, U. Catalytic Applications of Zeolites in Chemical Industry. *Top. Catal.* **2009**, *52*, 888–895. [CrossRef]

53. Wei, J.; Ge, Q.; Yao, R.; Wen, Z.; Fang, C.; Guo, L.; Xu, H.; Sun, J. Directly converting CO_2 into a gasoline fuel. *Nat. Commun.* **2017**, *8*, 15174, Erratum in **2017**, *8*, 16170. [CrossRef] [PubMed]

54. Popova, M.; Oykova, M.; Dimitrov, M.; Karashanova, D.; Kovacheva, D.; Atanasova, G.; Szegedi, Á. CO_2 Hydrogenation to Renewable Methane on Ni/Ru Modified ZSM-5 Zeolites: The Role of the Preparation Procedure. *Catalysts* **2022**, *12*, 1648. [CrossRef]

55. Bando, K.K.; Soga, K.; Kunimori, K.; Arakawa, H. Effect of Li additive on CO_2 hydrogenation reactivity of zeolite supported Rh catalysts. *Appl. Catal. A Gen.* **1998**, *175*, 67–81. [CrossRef]

56. Chan, B.; Radom, L. Design of Effective Zeolite Catalysts for the Complete Hydrogenation of CO_2. *J. Am. Chem. Soc.* **2006**, *128*, 5322–5323. [CrossRef] [PubMed]

57. Liu, R.; Leshchev, D.; Stavitski, E.; Juneau, M.; Agwara, J.N.; Porosoff, M.D. Selective hydrogenation of CO_2 and CO over potassium promoted Co/ZSM-5. *Appl. Catal. B Environ.* **2021**, *284*, 119787. [CrossRef]

58. Ramirez, A.; Chowdhury, A.D.; Dokania, A.; Cnudde, P.; Caglayan, M.; Yarulina, I.; Abou-Hamad, E.; Gevers, L.E.; Ould-Chikh, S.; De Wispelaere, K.; et al. Effect of Zeolite Topology and Reactor Configuration on the Direct Conversion of CO_2 to Light Olefins and Aromatics. *ACS Catal.* **2019**, *9*, 6320–6334. [CrossRef]

59. Pérez-Ramírez, J.; Christensen, C.H.; Egeblad, K.; Christensen, C.H.; Groen, J.C. Hierarchical zeolites: Enhanced utilisation of microporous crystals in catalysis by advances in materials design. *Chem. Soc. Rev.* **2008**, *37*, 2530–2542. [CrossRef] [PubMed]

60. Maghfirah, A.; Ilmi, M.; Fajar, A.; Kadja, G. A review on the green synthesis of hierarchically porous zeolite. *Mater. Today Chem.* **2020**, *17*, 100348. [CrossRef]

61. Song, G.; Li, M.; Yan, P.; Nawaz, M.A.; Liu, D. High Conversion to Aromatics via CO_2-FT over a CO-Reduced $Cu-Fe_2O_3$ Catalyst Integrated with HZSM-5. *ACS Catal.* **2020**, *10*, 11268–11279. [CrossRef]

62. Tian, H.; Gao, P.; Yang, X.; Jiao, C.; Zha, F.; Chang, Y.; Chen, H. Tandem composite of M (Zn, Ga, In)-UIO-66/(HZSM-5)-palygorskite for hydrogenation of carbon dioxide to aromatics. *Chem. Eng. J.* **2023**, *466*, 143267. [CrossRef]

63. Yan, P.; Peng, H.; Wu, X.; Rabiee, H.; Weng, Y.; Konarova, M.; Vogrin, J.; Rozhkovskaya, A.; Zhu, Z. Impact of varied zeolite materials on nickel catalysts in CO_2 methanation. *J. Catal.* **2024**, *432*, 115439. [CrossRef]

64. da Costa-Serra, J.F.; Cerdá-Moreno, C.; Chica, A. Zeolite-Supported Ni Catalysts for CO_2 Methanation: Effect of Zeolite Structure and Si/Al Ratio. *Appl. Sci.* **2020**, *10*, 5131. [CrossRef]

65. Bacariza, M.C.; Graca, I.; Lopes, J.M.; Henriques, C. Enhanced activity of CO_2 hydrogenation to CH_4 over Ni based zeolites through the optimization of the Si/Al ratio. *Microporous Mesoporous Mater.* **2018**, *267*, 9–19. [CrossRef]

66. Tada, S.; Li, D.; Okazaki, M.; Kinoshita, H.; Nishijima, M.; Yamauchi, N.; Kobayashi, Y.; Iyoki, K. Influence of Si/Al ratio of MOR type zeolites for bifunctional catalysts specific to the one-pass synthesis of lower olefins via CO_2 hydrogenation. *Catal. Today* **2023**, *411–412*, 113828. [CrossRef]

67. Cui, X.; Gao, P.; Li, S.; Yang, C.; Liu, Z.; Wang, H.; Zhong, L.; Sun, Y. Selective Production of Aromatics Directly from Carbon Dioxide Hydrogenation. *ACS Catal.* **2019**, *9*, 3866–3876. [CrossRef]

68. Wei, J.; Yao, R.; Ge, Q.; Xu, D.; Fang, C.; Zhang, J.; Xu, H.; Sun, J. Precisely regulating Brønsted acid sites to promote the synthesis of light aromatics via CO_2 hydrogenation. *Appl. Catal. B Environ.* **2021**, *283*, 119648. [CrossRef]

69. Xiang, M.; Shi, Z.; Zhang, X.; Gao, Z.; Guo, J.; Wu, Z.; Ma, S.; Bai, J.; Zhang, W.; Deng, Y.; et al. Facile synthesis of hierarchical SAPO-56 zeolite as a highly efficient catalyst for CO_2 hydrogenation to methanol. *Fuel* **2024**, *361*, 130663. [CrossRef]

70. Cui, W.-G.; Li, Y.-T.; Yu, L.; Zhang, H.; Hu, T.-L. Zeolite-Encapsulated Ultrasmall Cu/ZnO_x Nanoparticles for the Hydrogenation of CO_2 to Methanol. *ACS Appl. Mater. Interfaces* **2021**, *13*, 18693–18703. [CrossRef] [PubMed]

71. Ashford, B.; Poh, C.-K.; Ostrikov, K.; Chen, L.; Tu, X. Plasma-catalytic CO_2 hydrogenation to ethane in a dielectric barrier discharge reactor. *J. CO2 Util.* **2022**, *57*, 101882. [CrossRef]

72. Feliz, M.Q.; Polaert, I.; Ledoux, A.; Fernandez, C.; Azzolina-Jury, F. Influence of ionic conductivity and dielectric constant of the catalyst on DBD plasma-assisted CO_2 hydrogenation into methanol. *J. Phys. D Appl. Phys.* **2021**, *54*, 334003. [CrossRef]

73. Bacariza, M.; Biset-Peiró, M.; Graça, I.; Guilera, J.; Morante, J.; Lopes, J.; Andreu, T.; Henriques, C. DBD plasma-assisted CO_2 methanation using zeolite-based catalysts: Structure composition-reactivity approach and effect of Ce as promoter. *J. CO2 Util.* **2018**, *26*, 202–211. [CrossRef]

74. Chen, H.; Mu, Y.; Shao, Y.; Chansai, S.; Xu, S.; Stere, C.E.; Xiang, H.; Zhang, R.; Jiao, Y.; Hardacre, C.; et al. Coupling non-thermal plasma with Ni catalysts supported on BETA zeolite for catalytic CO_2 methanation. *Catal. Sci. Technol.* **2019**, *9*, 4135–4145. [CrossRef]

75. Jwa, E.; Lee, S.; Lee, H.; Mok, Y. Plasma-assisted catalytic methanation of CO and CO_2 over Ni–zeolite catalysts. *Fuel Process. Technol.* **2013**, *108*, 89–93. [CrossRef]

76. Da Costa, P.; Hasrack, G.; Bonnety, J.; Henriques, C. Ni-based catalysts for plasma-assisted CO_2 methanation. *Curr. Opin. Green Sustain. Chem.* **2021**, *32*, 100540. [CrossRef]

77. Medford, A.J.; Vojvodic, A.; Hummelshøj, J.S.; Voss, J.; Abild-Pedersen, F.; Studt, F.; Bligaard, T.; Nilsson, A.; Nørskov, J.K. From the Sabatier principle to a predictive theory of transition-metal heterogeneous catalysis. *J. Catal.* **2015**, *328*, 36–42. [CrossRef]

78. Henckel, D.; Saha, P.; Intia, F.; Taylor, A.K.; Baez-Cotto, C.; Hu, L.; Schellekens, M.; Simonson, H.; Miller, E.M.; Verma, S.; et al. Elucidation of Critical Catalyst Layer Phenomena toward High Production Rates for the Electrochemical Conversion of CO to Ethylene. *ACS Appl. Mater. Interfaces* **2024**, *16*, 3243–3252. [CrossRef] [PubMed]

79. Mitchell, S.; Pinar, A.B.; Kenvin, J.; Crivelli, P.; Kärger, J.; Pérez-Ramírez, J. Structural analysis of hierarchically organized zeolites. *Nat. Commun.* **2015**, *6*, 8633. [CrossRef] [PubMed]

80. Jacobsen, C.J.H.; Madsen, C.; Houzvicka, J.; Schmidt, I.; Carlsson, A. Mesoporous Zeolite Single Crystals. *J. Am. Chem. Soc.* **2000**, *122*, 7116–7117. [CrossRef]

81. Schmidt, I.; Boisen, A.; Gustavsson, E.; Ståhl, K.; Pehrson, S.; Dahl, S.; Carlsson, A.; Jacobsen, C.J.H. Carbon Nanotube Templated Growth of Mesoporous Zeolite Single Crystals. *Chem. Mater.* **2001**, *13*, 4416–4418. [CrossRef]

82. Chen, H.; Wydra, J.; Zhang, X.; Lee, P.-S.; Wang, Z.; Fan, W.; Tsapatsis, M. Hydrothermal Synthesis of Zeolites with Three-Dimensionally Ordered Mesoporous-Imprinted Structure. *J. Am. Chem. Soc.* **2011**, *133*, 12390–12393. [CrossRef] [PubMed]

83. Wu, J.; Jin, Z.; Wang, B.; Han, Y.; Xu, Y.; Liang, Z.; Wang, Z. Nickel Nanoparticles Encapsulated in Microporous Graphenelike Carbon (Ni@MGC) as Catalysts for CO_2 Methanation. *Ind. Eng. Chem. Res.* **2019**, *58*, 20536–20542. [CrossRef]

84. Pal, N.; Bhaumik, A. Soft templating strategies for the synthesis of mesoporous materials: Inorganic, organic–inorganic hybrid and purely organic solids. *Adv. Colloid Interface Sci.* **2013**, *189–190*, 21–41. [CrossRef] [PubMed]

85. Möller, K.; Yilmaz, B.; Müller, U.; Bein, T. Hierarchical Zeolite Beta via Nanoparticle Assembly with a Cationic Polymer. *Chem. Mater.* **2011**, *23*, 4301–4310. [CrossRef]

86. Kadja, G.T.; Suprianti, T.R.; Ilmi, M.M.; Khalil, M.; Mukti, R.R.; Subagjo. Sequential mechanochemical and recrystallization methods for synthesizing hierarchically porous ZSM-5 zeolites. *Microporous Mesoporous Mater.* **2020**, *308*, 110550. [CrossRef]

87. Xiao, F.; Wang, L.; Yin, C.; Lin, K.; Di, Y.; Li, J.; Xu, R.; Su, D.S.; Schlögl, R.; Yokoi, T.; et al. Catalytic Properties of Hierarchical Mesoporous Zeolites Templated with a Mixture of Small Organic Ammonium Salts and Mesoscale Cationic Polymers. *Angew. Chem.* **2006**, *118*, 3162–3165. [CrossRef]

88. Choi, M.; Cho, H.S.; Srivastava, R.; Venkatesan, C.; Choi, D.-H.; Ryoo, R. Amphiphilic organosilane-directed synthesis of crystalline zeolite with tunable mesoporosity. *Nat. Mater.* **2006**, *5*, 718–723. [CrossRef]

89. Pan, T.; Wu, Z.; Yip, A.C.K. Advances in the Green Synthesis of Microporous and Hierarchical Zeolites: A Short Review. *Catalysts* **2019**, *9*, 274. [CrossRef]

90. Tian, P.; Zhan, G.; Tian, J.; Tan, K.B.; Guo, M.; Han, Y.; Fu, T.; Huang, J.; Li, Q. Direct CO_2 hydrogenation to light olefins over ZnZrO$_x$ mixed with hierarchically hollow SAPO-34 with rice husk as green silicon source and template. *Appl. Catal. B Environ.* **2022**, *315*, 121572. [CrossRef]

91. Din, I.U.; Din, I.U.; Alotaibi, M.A.; Alotaibi, M.A.; Alharthi, A.I.; Alharthi, A.I.; Al-Shalwi, M.N.; Al-Shalwi, M.N.; Alshehri, F.; Alshehri, F. Green synthesis approach for preparing zeolite based Co-Cu bimetallic catalysts for low temperature CO_2 hydrogenation to methanol. *Fuel* **2022**, *330*, 125643. [CrossRef]

92. Gourdon, A. On-Surface Covalent Coupling in Ultrahigh Vacuum. *Angew. Chem. Int. Ed.* **2008**, *47*, 6950–6953. [CrossRef] [PubMed]

93. Debecker, D.P.; Le Bras, S.; Boissière, C.; Chaumonnot, A.; Sanchez, C. Aerosol processing: A wind of innovation in the field of advanced heterogeneous catalysts. *Chem. Soc. Rev.* **2018**, *47*, 4112–4155. [CrossRef] [PubMed]

94. Thilakarajan, P. Synthesis and Evaluation of Nanocatalysts for CO_2 Hydrogenation to Methanol: A Comprehensive Review. *Int. J. High Sch. Res.* **2024**, *6*, 118–126.

95. Bahari, N.A.; Isahak, W.N.R.W.; Ba-Abbad, M.M. The Effectiveness of Various Bimetallic on Iron-Zeolite Catalyst by Carbon Dioxide Hydrogenation. *IOP Conf. Ser. Earth Environ. Sci.* **2019**, *268*, 012110. [CrossRef]

96. Gao, X.; Deng, S.; Kawi, S. Zeolite-based catalytic membrane reactors for thermo-catalytic conversion of CO_2. *iScience* **2022**, *25*, 105343. [CrossRef] [PubMed]

97. Maghfirah, A.; Susanti, Y.; Fajar, A.T.N.; Mukti, R.R.; Kadja, G.T.M. The role of tetraalkylammonium for controlling dealumination of zeolite Y in acid media. *Mater. Res. Express* **2019**, *6*, 094002. [CrossRef]

98. Fajar, A.; Nurdin, F.; Mukti, R.; Subagjo; Rasrendra, C.; Kadja, G. Synergistic effect of dealumination and ceria impregnation to the catalytic properties of MOR zeolite. *Mater. Today Chem.* **2020**, *17*, 100313. [CrossRef]

99. Le Hua, Z.; Zhou, J.; Shi, J.L. Recent advances in hierarchically structured zeolites: Synthesis and material performances. *Chem. Commun.* **2011**, *47*, 10536–10547. [CrossRef]

100. Verboekend, D.; Mitchell, S.; Milina, M.; Groen, J.C.; Pérez-Ramírez, J. Full Compositional Flexibility in the Preparation of Mesoporous MFI Zeolites by Desilication. *J. Phys. Chem. C* **2011**, *115*, 14193–14203. [CrossRef]

101. Wardani, M.K.; Kadja, G.T.M.; Fajar, A.T.N.; Subagjo, S.; Makertihartha, I.G.B.N.; Gunawan, M.L.; Suendo, V.; Mukti, R.R. Highly crystalline mesoporous SSZ-13 zeolite obtained via controlled post-synthetic treatment. *RSC Adv.* **2019**, *9*, 77–86. [CrossRef] [PubMed]

102. Wakihara, T.; Tatami, J. Top-down Tuning of Nanosized Zeolites by Bead-milling and Recrystallization. *J. Jpn. Pet. Inst.* **2013**, *56*, 206–213. [CrossRef]

103. Kurniawan, T.; Muraza, O.; Hakeem, A.S.; Al-Amer, A.M. Mechanochemical Route and Recrystallization Strategy To Fabricate Mordenite Nanoparticles from Natural Zeolites. *Cryst. Growth Des.* **2017**, *17*, 3313–3320. [CrossRef]

104. Airi, A.; Signorile, M.; Bonino, F.; Quagliotto, P.; Bordiga, S.; Martens, J.A.; Crocellà, V. Insights on a Hierarchical MFI Zeolite: A Combined Spectroscopic and Catalytic Approach for Exploring the Multilevel Porous System Down to the Active Sites. *ACS Appl. Mater. Interfaces* **2021**, *13*, 49114–49127. [CrossRef]

105. Jia, X.; Khan, W.; Wu, Z.; Choi, J.; Yip, A.C. Modern synthesis strategies for hierarchical zeolites: Bottom-up versus top-down strategies. *Adv. Powder Technol.* **2019**, *30*, 467–484. [CrossRef]

106. Dapsens, P.Y.; Mondelli, C.; Pérez-Ramírez, J. Design of Lewis-acid centres in zeolitic matrices for the conversion of renewables. *Chem. Soc. Rev.* **2015**, *44*, 7025–7043. [CrossRef] [PubMed]

107. Ding, L.; Shi, T.; Gu, J.; Cui, Y.; Zhang, Z.; Yang, C.; Chen, T.; Lin, M.; Wang, P.; Xue, N.; et al. CO_2 Hydrogenation to Ethanol over Cu@Na-Beta. *Chem* **2020**, *6*, 2673–2689. [CrossRef]

108. Bacariza, M.C.; Graça, I.; Westermann, A.; Ribeiro, M.F.; Lopes, J.M.; Henriques, C. CO_2 Hydrogenation Over Ni-Based Zeolites: Effect of Catalysts Preparation and Pre-reduction Conditions on Methanation Performance. *Top. Catal.* **2016**, *59*, 314–325. [CrossRef]

109. Bacariza, M.C.; Graça, I.; Lopes, J.M.; Henriques, C. Tuning Zeolite Properties towards CO_2 Methanation: An Overview. *ChemCatChem* **2019**, *11*, 2388–2400. [CrossRef]

110. Verboekend, D.; Pérez-Ramírez, J. Design of hierarchical zeolite catalysts by desilication. *Catal. Sci. Technol.* **2011**, *1*, 879–890. [CrossRef]

111. Gackowski, M.; Tarach, K.; Kuterasiński, Ł.; Podobiński, J.; Sulikowski, B.; Datka, J. Spectroscopic IR and NMR studies of hierarchical zeolites obtained by desilication of zeolite Y: Optimization of the desilication route. *Microporous Mesoporous Mater.* **2019**, *281*, 134–141. [CrossRef]

112. Dai, C.; Zhang, A.; Li, L.; Hou, K.; Ding, F.; Li, J.; Mu, D.; Song, C.; Liu, M.; Guo, X. Synthesis of Hollow Nanocubes and Macroporous Monoliths of Silicalite-1 by Alkaline Treatment. *Chem. Mater.* **2013**, *25*, 4197–4205. [CrossRef]

113. Sharma, P.; Ho, P.H.; Di, W.; Creaser, D.; Olsson, L. Novel catalyst configuration to boost the yield of longer hydrocarbons from methanol-mediated CO_2 hydrogenation. *J. CO2 Util.* **2023**, *74*, 102549. [CrossRef]

114. Gac, W.; Zawadzki, W.; Słowik, G.; Kuśmierz, M.; Dzwigaj, S. The state of BEA zeolite supported nickel catalysts in CO_2 methanation reaction. *Appl. Surf. Sci.* **2021**, *564*, 150421. [CrossRef]

115. Krachuamram, S.; Kidkhunthod, P.; Poo-Arporn, Y.; Kamonsutthipaijit, N.; Chanapattharapol, K.C. On the Optimization of Ni/A and Ni/X Synthesis Procedure toward Active and Selective Catalysts for the Production of CH_4 from CO_2. *Catalysts* **2022**, *12*, 823. [CrossRef]

116. Velisoju, V.K.; Cerrillo, J.L.; Ahmad, R.; Mohamed, H.O.; Attada, Y.; Cheng, Q.; Yao, X.; Zheng, L.; Shekhah, O.; Telalovic, S.; et al. Copper nanoparticles encapsulated in zeolitic imidazolate framework-8 as a stable and selective CO_2 hydrogenation catalyst. *Nat. Commun.* **2024**, *15*, 2045. [CrossRef]

117. Ticali, P.; Salusso, D.; Ahmad, R.; Ahoba-Sam, C.; Ramirez, A.; Shterk, G.; Lomachenko, K.A.; Borfecchia, E.; Morandi, S.; Cavallo, L.; et al. CO_2 hydrogenation to methanol and hydrocarbons over bifunctional Zn-doped ZrO_2/zeolite catalysts. *Catal. Sci. Technol.* **2021**, *11*, 1249–1268. [CrossRef]

118. Wang, X.; Jeong, S.Y.; Jung, H.S.; Shen, D.; Ali, M.; Zafar, F.; Chung, C.-H.; Bae, J.W. Catalytic activity for direct CO_2 hydrogenation to dimethyl ether with different proximity of bifunctional Cu-ZnO-Al_2O_3 and ferrierite. *Appl. Catal. B Environ.* **2023**, *327*, 122456. [CrossRef]

119. Wang, C.; Guan, E.; Wang, L.; Chu, X.; Wu, Z.; Zhang, J.; Yang, Z.; Jiang, Y.; Zhang, L.; Meng, X.; et al. Product Selectivity Controlled by Nanoporous Environments in Zeolite Crystals Enveloping Rhodium Nanoparticle Catalysts for CO_2 Hydrogenation. *J. Am. Chem. Soc.* **2019**, *141*, 8482–8488. [CrossRef] [PubMed]

120. Dang, S.; Gao, P.; Liu, Z.; Chen, X.; Yang, C.; Wang, H.; Zhong, L.; Li, S.; Sun, Y. Role of zirconium in direct CO_2 hydrogenation to lower olefins on oxide/zeolite bifunctional catalysts. *J. Catal.* **2018**, *364*, 382–393. [CrossRef]